

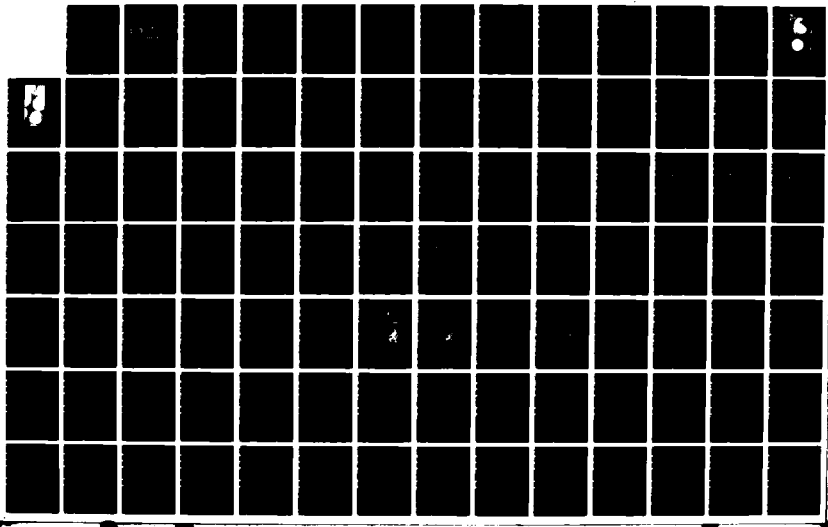
HD-4195-446 2-DIMENSIONAL AXISYMMETRIC AND 3-DIMENSIONAL FINITE  
ELEMENT STRESS ANALYSIS OF THE LHA-1 CLASS SUPERHEATER  
HEADER(U) NAVAL POSTGRADUATE SCHOOL MONTEREY CA

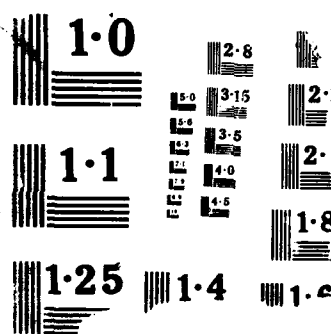
UNCLASSIFIED D R KITCHIN MAR 88

1A

F/G 28/11

NL





AD-A195 446

(2)

# NAVAL POSTGRADUATE SCHOOL

Monterey, California

DTIC  
ELECTED  
JUL 08 1988  
CD



## THESIS

2-DIMENSIONAL AXISYMMETRIC AND  
3-DIMENSIONAL FINITE ELEMENT  
STRESS ANALYSIS OF THE LHA-1 CLASS SUPER-  
HEATER HEADER

by

Doyle R. Kitchin

March 1988

Thesis Advisor

G. Cantin

Approved for public release; distribution is unlimited.

Unclassified

security classification of this page

REPORT DOCUMENTATION PAGE

1a Report Security Classification Unclassified		1b Restrictive Markings	
2a Security Classification Authority		3 Distribution Availability of Report Approved for public release; distribution is unlimited.	
2b Declassification Downgrading Schedule			
4 Performing Organization Report Number(s)		5 Monitoring Organization Report Number(s)	
6a Name of Performing Organization Naval Postgraduate School	6b Office Symbol (if applicable) 69	7a Name of Monitoring Organization Naval Postgraduate School	
6c Address (city, state, and ZIP code) Monterey, CA 93943-5000		7b Address (city, state, and ZIP code) Monterey, CA 93943-5000	
8a Name of Funding Sponsoring Organization	8b Office Symbol (if applicable)	9 Procurement Instrument Identification Number	
10c Address (city, state, and ZIP code)		10 Source of Funding Numbers Program Element No Project No Task No Work Unit Accession No	

11 Title (include security classification) 2-DIMENSIONAL AXISYMMETRIC AND 3-DIMENSIONAL FINITE ELEMENT STRESS ANALYSIS OF THE LHA-1 CLASS SUPERHEATER HEADER

12 Personal Author(s) Doyle R. Kitchin

13a Type of Report Master's Thesis	13b Time Covered From _____ To _____	14 Date of Report (year, month, day) March 1988	15 Page Count 112
---------------------------------------	---	--	----------------------

16 Supplementary Notation The views expressed in this thesis are those of the author and do not reflect the official policy or position of the Department of Defense or the U.S. Government.

17 Categorical Codes			18 Subject Terms (continue on reverse if necessary and identify by block number)
Field	Group	Subgroup	Thermal Stress Analysis

19 Abstract (continue on reverse if necessary and identify by block number)

ADINA, a finite element program for automatic dynamic incremental nonlinear analysis, is used to conduct a stress analysis of the Tarawa class (LHA-1) superheater header. This investigation is sponsored by the Naval Sea Systems Command (NAVSEA) as a result of cracking in the superheater header tube attachment weld. A 2-dimensional solid axisymmetric finite element model was developed using both a coarse and fine mesh. Both pressure and thermally induced stresses were studied. A 3-dimensional solid finite element model was developed and a preliminary stress analysis conducted.

The report  
11

20 Distribution Availability of Abstract <input checked="" type="checkbox"/> unclassified/unlimited <input type="checkbox"/> same as report <input type="checkbox"/> DDCI users	21 Abstract Security Classification Unclassified	
22a Name of Responsible Individual G. Cantin	22b Telephone (include Area code) (408) 646-2364	22c Office Symbol 69Ci

DD FORM 1473,34 MAR

83 APR edition may be used until exhausted  
All other editions are obsolete

security classification of this page

Unclassified

Approved for public release; distribution is unlimited.

2-dimensional axisymmetric and 3-dimensional finite element  
stress analysis of the LHA-1 class superheater header

by

Doyle R. Kitchin  
Lieutenant Commander, United States Navy  
B.S.M.E., United States Naval Academy, 1976

Submitted in partial fulfillment of the  
requirements for the degrees of

MASTER OF SCIENCE IN MECHANICAL ENGINEERING  
and  
MECHANICAL ENGINEER

from the

NAVAL POSTGRADUATE SCHOOL  
March 1988

Author:

Doyle R. Kitchin

Doyle R. Kitchin

Approved by:

Gilles Cantin

G. Cantin, Thesis Advisor

D. Salinas

D. Salinas, Second Reader

A.J. Healey

A.J. Healey, Chairman,  
Department of Mechanical Engineering

G. Schacher

Gordon E. Schacher,  
Dean of Science and Engineering

## ABSTRACT

ADINA, a finite element program for automatic dynamic incremental nonlinear analysis, is used to conduct a stress analysis of the Tarawa class (LHA-1) superheater header. This investigation is sponsored by the Naval Sea Systems Command (NAVSEA) as a result of cracking in the superheater header tube attachment weld. A 2-dimensional solid axisymmetric finite element model was developed using both a coarse and fine mesh. Both pressure and thermally induced stresses were studied. A 3-dimensional solid finite element model was developed and a preliminary stress analysis conducted.

Accession For	
NTIS CRA&I	<input checked="" type="checkbox"/>
DTIC TAB	<input type="checkbox"/>
Unpublished	<input type="checkbox"/>
JASPER	<input type="checkbox"/>
By _____	
Distribution / _____	
Availability Codes	
Dist	Aval and/or Special
A-1	



## TABLE OF CONTENTS

I.	INTRODUCTION .....	1
II.	DESCRIPTION OF THE PROBLEM .....	2
III.	DESCRIPTION OF ADINA .....	5
A.	GENERATION OF INPUT DATA .....	5
B.	POST-PROCESSING .....	5
C.	METHOD OF SOLUTION .....	7
D.	AXISYMMETRIC PROBLEM .....	8
E.	CONTACT SURFACES .....	9
F.	THERMAL ANALYSIS .....	9
G.	VERIFICATION .....	11
IV.	2-DIMENSIONAL SOLID AXISYMMETRIC FINITE ELEMENT MODEL	12
A.	INITIAL MODEL DEVELOPMENT .....	12
B.	LOAD CONDITIONS .....	12
1.	Load condition no. 1 - Internal pressure load .....	12
2.	Load condition no. 2 - Longitudinal tube load .....	22
3.	Load condition no. 3 - Thermal load .....	22
C.	MATERIAL PROPERTIES .....	22
D.	COMPARISON OF RESULTS .....	22
E.	FURTHER MODEL DEVELOPMENT .....	36
F.	THERMAL GRADIENTS. ....	37
V.	3-DIMENSIONAL SOLID FINITE ELEMENT MODEL .....	48
A.	MODEL DEVELOPMENT .....	48
B.	INTERNAL PRESSURE LOAD .....	48
VI.	CONCLUSIONS .....	61
A.	DISCUSSION OF RESULTS .....	61
B.	OPPORTUNITIES FOR FURTHER RESEARCH .....	61

APPENDIX A. ADINA-IN PROCEDURES .....	62
APPENDIX B. ADINA-IN PROCEDURES FOR THE THERMAL STRESS PROBLEM .....	63
APPENDIX C. ADINA-PLOT PROCEDURES .....	64
APPENDIX D. VERIFICATION OF ADINA - CANTILEVER BEAM PROBLEM .....	65
APPENDIX E. VERIFICATION OF ADINA - ANNULAR DISK PROBLEM .....	69
APPENDIX F. VERIFICATION OF ADINA - CHIMNEY PROBLEM .....	72
APPENDIX G. ADINA-IN INPUT FILE FOR THE AXISYMMETRIC PROBLEM .....	76
APPENDIX H. ADINA-IN INPUT FILE FOR THE 3-DIMENSIONAL CONTACT SURFACE .....	82
APPENDIX I. ADINA-IN INPUT FILE FOR THE 3-DIMENSIONAL PROBLEM .....	87
LIST OF REFERENCES .....	101
INITIAL DISTRIBUTION LIST .....	102

## LIST OF TABLES

Table 1. MAXIMUM STRESSES FOR THE COARSE MESH .....	32
Table 2. MAXIMUM STRESSES FOR THE FINE MESH .....	32
Table 3. PRINCIPAL STRESSES FOR THE COARSE MESH .....	32
Table 4. PRINCIPAL STRESSES FOR THE FINE MESH .....	33
Table 5. MAXIMUM STRESSES FOR THE COARSE MESH, CONTACT SURFACE OPTION .....	36
Table 6. MAXIMUM STRESSES FOR THE FINE MESH, CONTACT SUR- FACE OPTION .....	36
Table 7. MAXIMUM STRESSES FOR THE COARSE MESH, REPEATING SECTION .....	37
Table 8. MAXIMUM STRESSES FOR THE FINE MESH, REPEATING SEC- TION .....	37
Table 9. MAXIMUM STRESSES FOR DIFFERENT THERMAL GRADIENTS	44
Table 10. MAXIMUM STRESSES FOR THE COARSE MESH, EXPANDING RADIALLY .....	47
Table 11. MAXIMUM STRESSES 3-DIMENSIONAL MODEL .....	59
Table 12. COMPARISON OF RESULTS .....	65
Table 13. COMPARISON OF RESULTS .....	69
Table 14. RESULTS FOR CHIMNEY PROBLEM .....	72

## LIST OF FIGURES

Figure 1.	Magnetic particle indications of transverse weld cracks in no. 2 boiler intermediate header tube .....	3
Figure 2.	Magnetic particle indications of ligament cracks in no. 1 boiler inlet/outlet header tube attachment joints .....	4
Figure 3.	Sequence of execution of ADINA programs .....	6
Figure 4.	Contact surface contactor segment .....	10
Figure 5.	Cross sectional view of the superheater header .....	13
Figure 6.	Detail of the attachment weld joint .....	14
Figure 7.	Geometry of the weld .....	15
Figure 8.	Coarse mesh .....	16
Figure 9.	Close-up of the weld area, coarse mesh .....	17
Figure 10.	Fine mesh .....	18
Figure 11.	Close-up of the weld area, fine mesh .....	19
Figure 12.	Fixed boundary conditions .....	20
Figure 13.	Load condition no. 1 .....	21
Figure 14.	Load condition no. 2, coarse mesh .....	23
Figure 15.	Load condition no. 2, fine mesh .....	24
Figure 16.	Load condition no. 3 .....	25
Figure 17.	Original and deformed shape of coarse mesh for load condition no. 1 ..	26
Figure 18.	Original and deformed shape of coarse mesh for load condition no. 2 ..	27
Figure 19.	Original and deformed shape of coarse mesh for load condition no. 3 ..	28
Figure 20.	Original and deformed shape of fine mesh for load condition no. 1 ..	29
Figure 21.	Original and deformed shape of fine mesh for load condition no. 2 ..	30
Figure 22.	Original and deformed shape of fine mesh for load condition no. 3 ..	31
Figure 23.	Vector plot of the principal stresses of the coarse mesh for load condition no. 3 ..	34
Figure 24.	Vector plot of the principal stresses of the fine mesh for load condition no. 3 ..	35
Figure 25.	Coarse mesh, repeating section .....	38
Figure 26.	Fine mesh, repeating section .....	39
Figure 27.	Rolling boundary conditions .....	40

Figure 28. Original and deformed shape of coarse mesh for load condition no. 1, repeating section .....	41
Figure 29. Original and deformed shape of coarse mesh for load condition no. 2, repeating section .....	42
Figure 30. Original and deformed shape of coarse mesh for load condition no. 3, repeating section .....	43
Figure 31. Bottom rolling boundary condition .....	45
Figure 32. Original and deformed shape of the fine mesh for load condition no. 3, expanding radially and axially .....	46
Figure 33. 20-node isoparametric solid element .....	49
Figure 34. Mesh for one tube .....	50
Figure 35. Attachment of header to a tube .....	51
Figure 36. 3-dimensional model .....	52
Figure 37. 3-dimensional model showing the location of the origin .....	53
Figure 38. View of 3-dimensional model from the x direction .....	54
Figure 39. View of 3-dimensional model from the y direction .....	55
Figure 40. View of 3-dimensional model from the z direction .....	56
Figure 41. View of model using hidden line removal .....	57
Figure 42. Another view of the model using hidden line removal .....	58
Figure 43. Original and deformed shape of the 3-dimensional model, internal pressure load .....	60
Figure 44. Cantilever beam with concentrated moment .....	66
Figure 45. Original and deformed shapes for the cantilever beam .....	67
Figure 46. Original and deformed shapes for the disk .....	70
Figure 47. Chimney problem .....	73
Figure 48. Finite element model of the chimney .....	74

## I. INTRODUCTION

The Tarawa (LHA-1) class amphibious assault ships have been experiencing numerous failures of their superheater header. The failures occur in the tube attachment weld. This is a relatively new class of ship and they are expected to be in commission for another twenty to thirty years. The solution of this problem is imperative to prevent the excessive down time experienced by these engineering plants.

A 2-dimensional solid axisymmetric finite element model was developed using ADINA. A study of the effect of different thermal gradients across the thickness of the header was conducted. The model yielded very different results dependent on the boundary conditions imposed. A discussion is made of the boundary conditions and the conclusion that a 3-dimensional model would more closely model the actual physical boundary conditions of this structure.

A 3-dimensional solid finite element model was developed. A discussion is made of the boundary conditions and a study is made of the internal pressure loading.

## II. DESCRIPTION OF THE PROBLEM

NAVSEA has been conducting an extensive investigation to determine the cause for the weld joint cracking. The following list was provided by NAVSEA and is an analysis of weld joint cracking on the USS Tarawa (LHA-1):

- Linear defects were located by MT inspection in original fabrication welds and repair welds alike, including welds installed as recently as 1982.
- Predominant linear defect was the transverse weld crack, occurring singly and in multiples of two or more; crack indications ranged from 1 1/16 inch to 5 8/16 inch in length.
- Numerous linear indications were also found across the thin ligaments between welds in the A-to-D loop direction; cracks occurred singly and in multiples, and ranged in length from 1 1/16 inch to 3 1/4 inch.
- Predominant crack orientation was transverse to the longitudinal axis of the header; very few axially oriented indications were observed.
- Cracked welds in the inlet/outlet header were concentrated in the first and fourth passes.
- No apparent concentration of defects in the welds adjacent to the division plates (region of highest thermal gradient).
- The inlet/outlet header examined contained nearly 2-1/2 times as many weld joints with linear defects as did the intermediate header (32% of welds in no. 1 boiler inlet/outlet header vs. 13% of welds in no. 2 boiler intermediate header).
- Destructive analysis indicated the maximum crack depth to be approximately 5 3/32 inch, and the crack propagation mechanism to be fatigue at elevated temperature.

Figure 1 on page 3 and Figure 2 on page 4 are photographs taken by NAVSEA showing magnetic particle indications of the cracking. A more detailed description of this problem is given in [Ref. 1: pp. 10-15].



Figure 1. Magnetic particle indications of transverse weld cracks in no. 2 boiler intermediate header tube



Figure 2. Magnetic particle indications of ligament cracks in no. 1 boiler inlet/outlet header tube attachment joints

### III. DESCRIPTION OF ADINA

ADINA is a finite element program for automatic dynamic incremental nonlinear analysis. The ADINA system is composed of four main programs: ADINA-IN, ADINA, ADINA-PLOT and ADINAT. The 1984 version was used for this thesis. The sequence of execution of these programs is shown in Figure 3 on page 6 which is taken from [Ref. 2: p. 1-2].

#### A. GENERATION OF INPUT DATA

ADINA-IN generates the input data for ADINA or ADINAT. ADINA is used for displacement and stress analysis and ADINAT performs the temperature analysis. ADINA-IN can be run in an interactive or batch mode.

Coordinates can be input in a local or global coordinate system using cartesian, cylindrical or spherical coordinates. There are several automatic mesh generation methods available.

ADINA-IN has the ability to graphically check the model. All or part of the model can be drawn from any view desired, including element and nodal numbering. The LINES parameter described in [Ref. 2: p. 5.25-15] gives some ability to specify which lines on the model will be drawn. This allows an outline of the model to be drawn and the ability to check for missing elements.

The procedure for utilizing ADINA-IN to generate input data for ADINA on the VAX/VMS operating system is explained in Appendix A. The procedure for utilizing ADINA-IN to generate input data to solve the thermally induced stress problem is explained in Appendix B. The reverse Cuthill-McKee bandwidth optimization is used in generating the input file for ADINA.

#### B. POST-PROCESSING

ADINA-PLOT performs the post-processing of the output data from ADINA. It also has graphics capability, allowing a view of both the deformed and undeformed shapes. The deformed scale factor can be specified. ADINA-PLOT can also do vector plotting of the principal stresses.

Several listing options are available. Displacements or stresses for all or part of the model can be printed. Maximum values or results exceeding a specified value can also be listed.

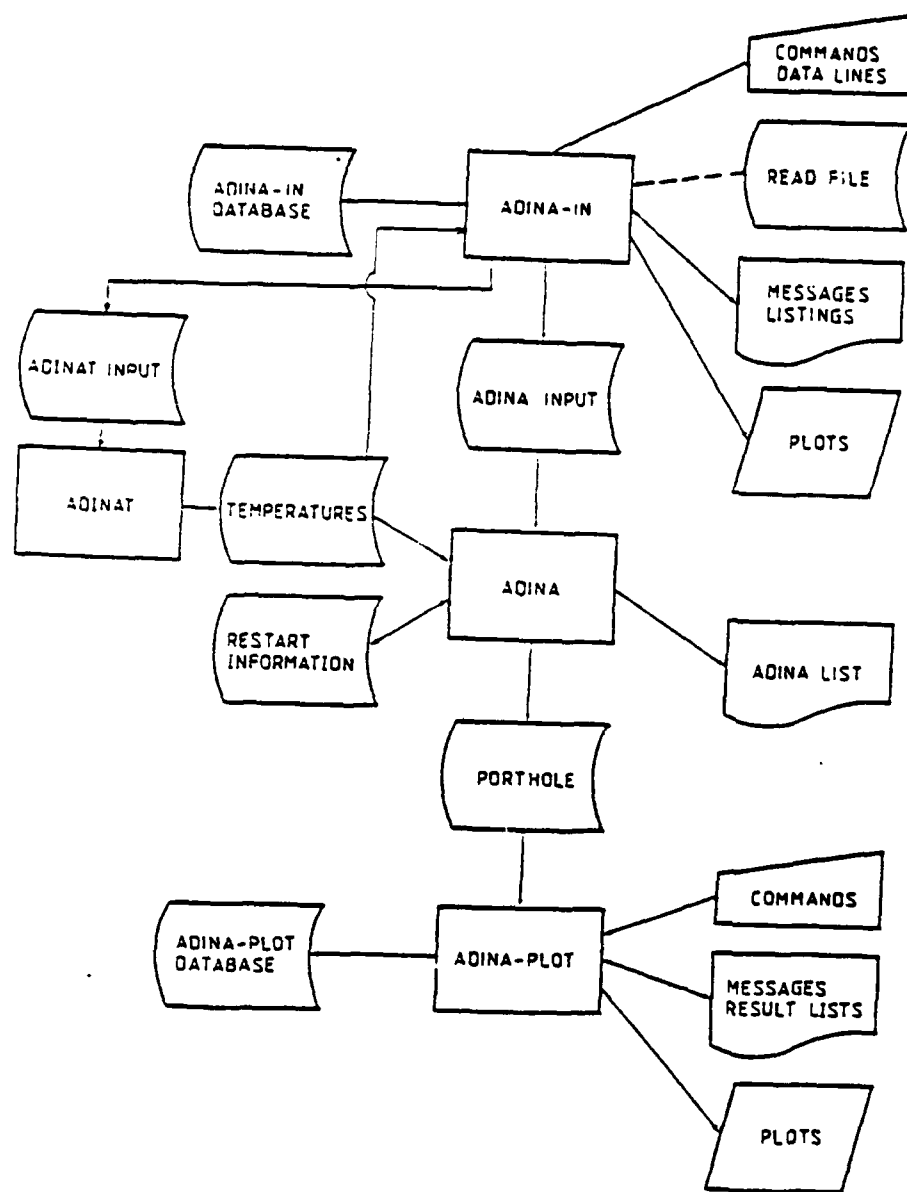


Figure 3. Sequence of execution of ADINA programs

The procedure for operating ADINA-PLOT on the VAX/VMS operating system is explained in Appendix C.

### C. METHOD OF SOLUTION

ADINA uses isoparametric displacement based finite elements. The basic assumptions from [Ref. 3: p. 2.3-8] are:

for the coordinates

$$x = \sum_{i=1}^q h_i x_i \quad y = \sum_{i=1}^q h_i y_i \quad z = \sum_{i=1}^q h_i z_i \quad (3.1)$$

for the displacements

$$u = \sum_{i=1}^q h_i u_i \quad v = \sum_{i=1}^q h_i v_i \quad w = \sum_{i=1}^q h_i w_i \quad (3.2)$$

where:

- $h_i(r,s,t)$  = the interpolation function corresponding to node i
- $r,s,t$  = the isoparametric coordinates
- $q$  = the number of element nodes
- $x_i, y_i, z_i$  = nodal point coordinates
- $u_i, v_i, w_i$  = nodal point displacements

ADINA uses the principle of virtual displacement to generate the equilibrium equations. The equilibrium equation as listed in [Ref. 4: p. 124] is:

$$K U = R \quad (3.3)$$

where:

- $K$  = the element stiffness matrix
- $U$  = the unknown nodal point displacements
- $R$  = the load vector which includes body forces, surface forces, initial stresses and concentrated loads.

The development of the stiffness matrix for the isoparametric element is given in [Ref. 4: pp. 203-204]:

$$K = \int_V B^T C B dV \quad (3.4)$$

where:

- $B$  = the strain-displacement matrix
- $C$  = the elasticity matrix

In terms of the isoparametric coordinates:

$$dV = \det(J) dr ds dt \quad (3.5)$$

where:

- $\det(J)$  = the determinant of the Jacobian operator

The stresses are calculated using the strains at the point of interest. The basic relationships used are given in [Ref. 4: p. 123]:

$$\varepsilon = B U \quad (3.6)$$

$$\tau = C \varepsilon \quad (3.7)$$

where:

- $\varepsilon$  = the element strain matrix
- $\tau$  = the element stress matrix

The element matrices are calculated using Gauss numerical integration. A (3x3x3) integration order is utilized as specified in [Ref. 3 : p. 2.3-16].

#### D. AXISYMMETRIC PROBLEM

The basic assumptions for the axisymmetric element are listed in [Ref. 3: p. 2.2-4]:

$$\varepsilon_{xx} = u/y \quad (x \text{ is the hoop direction}) \quad (3.8)$$

$$\tau_{xy} = \tau_{xz} = 0 \quad (y \text{ is the radial direction}) \quad (3.9)$$

If the loading is also axisymmetric, a 2-dimensional analysis of a unit radian of the structure will provide the complete stress and strain distributions. This greatly reduces the computational time compared to a 3-dimensional analysis.

## E. CONTACT SURFACES

ADINA allows the specification of contact surfaces in the development of the model. Contact surfaces are defined in [Ref. 3: p. 4.1-1] as surfaces that are initially in contact, or are anticipated to come into contact during the response solution.

The contact surface problem is a nonlinear analysis. After each equilibrium iteration, the segment contact force is evaluated from the nodal forces. A contactor segment is shown in Figure 4 on page 10. The conditions of either tension release, sliding or sticking are determined for each segment. The basic equations are given in [Ref. 3: p. 4.2-3]. Tension release occurs if:

$$\vec{\eta} \cdot \vec{T}_n^j < 0 \quad (3.10)$$

where:

- $\vec{\eta}$  = the inward normal vector to segment j as shown in Figure 4 on page 10
- $\vec{T}_n^j$  = the normal contact force for segment j

Tension release means the surfaces are not in contact.

If the surfaces are in contact the condition of sliding or sticking is determined by using the friction law. Sticking occurs if:

$$\vec{T}_t^j < \mu \vec{T}_n^j \quad (3.11)$$

where:

- $\vec{T}_t^j$  = the tangential contact force for segment j
- $\mu$  = the coefficient of friction

Sliding occurs if:

$$\vec{T}_t^j > \mu \vec{T}_n^j \quad (3.12)$$

The nodal forces are calculated as the consistent nodal loads which correspond to the tangential and normal forces of the segment.

## F. THERMAL ANALYSIS

ADINAT uses isoparametric finite element discretization. The basic assumptions from [Ref. 5: p. 11] are:

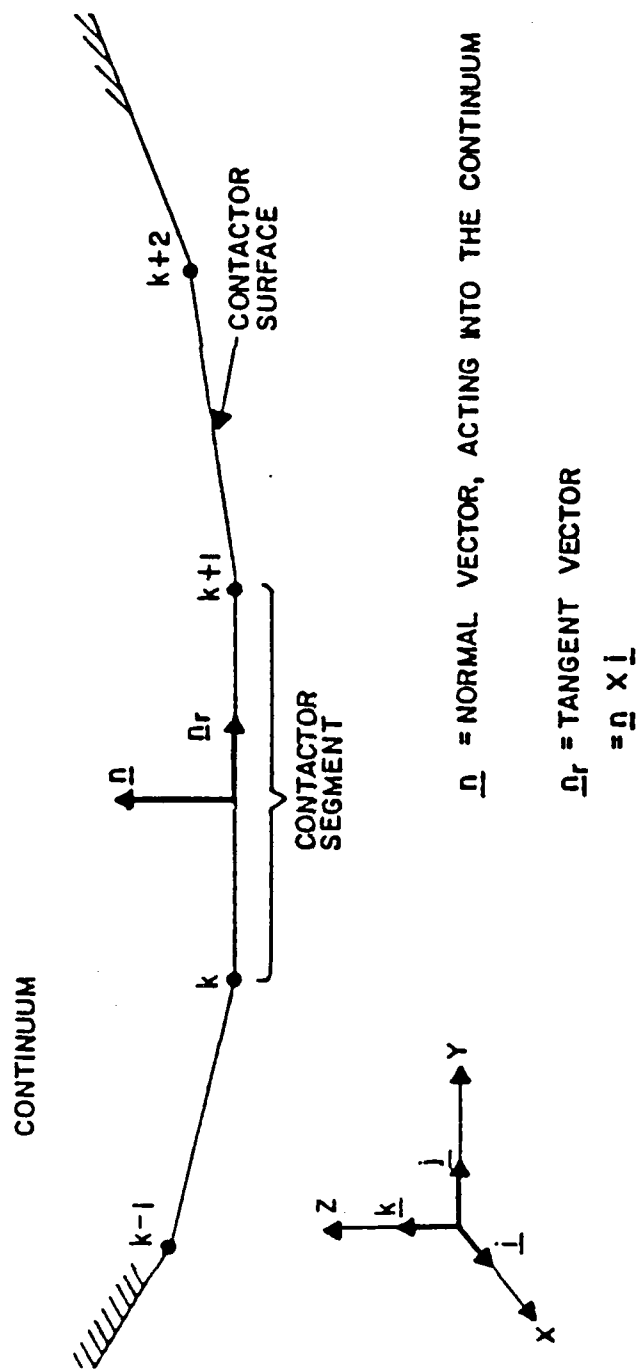


Figure 4. Contact surface contacter segment

$$x = \sum_{i=1}^N h_i x_i \quad y = \sum_{i=1}^N h_i y_i \quad z = \sum_{i=1}^N h_i z_i \quad (3.13)$$

and:

$$t + \Delta t_{\theta} = \sum_{i=1}^N h_i t + \Delta t_{\theta,i} \quad t_{\theta} = \sum_{i=1}^N h_i t_{\theta,i} \quad \Delta \theta = \sum_{i=1}^N h_i \Delta \theta_i \quad (3.14)$$

where:

- $h_i$  = the element interpolation function
- $N$  = the number of nodal points
- $x_i, y_i, z_i$  = coordinates of the nodal point i
- $t + \Delta t_{\theta,i}$  = the temperature of nodal point i at time  $t + \Delta t$
- $t_{\theta,i}$  = the temperature of nodal point i at time t
- $\Delta \theta_i$  = the temperature increment at nodal point i

The interpolation and substitution of these equations into the general incremental heat flow equilibrium equations yield the finite element equations.

#### G. VERIFICATION

Part of the installation process of a finite element code is the verification of the code. This is done by modeling a problem for which the results are known and comparing the results.

Three verifications are included in this thesis. The solution of a cantilever beam problem is compared with classical beam theory in Appendix D. The thermal stresses in an annular disk are compared with classical disk theory in Appendix E. The temperature distribution in a chimney is compared with a verified finite difference solution in Appendix F. The last two problems were chosen because of their similarity to the problem addressed in this thesis. In each case ADINA yielded excellent results.

## IV. 2-DIMENSIONAL SOLID AXISYMMETRIC FINITE ELEMENT MODEL

This problem was originally modeled by Lieutenant Jon W. Kaufmann, United States Navy, in [Ref. 1]. The initial attempt of this thesis was to duplicate his model.

### A. INITIAL MODEL DEVELOPMENT

NAVSEA provided a cross section drawing of the superheater header as illustrated in Figure 5 on page 13. They also provided a detail of the superheater header tube attachment weld joint in Figure 6 on page 14. The same geometry of the weld as developed in [Ref. 1: p. 18] was utilized and is illustrated in Figure 7 on page 15.

A nine-node plane axisymmetric element was used. This element is similar to the one used in [Ref. 1: p. 29].

A coarse and fine mesh were developed in order to do a study on convergence. The coarse mesh has 64 elements and 292 nodes. The model is shown in Figure 8 on page 16. A close-up of the weld is shown in Figure 9 on page 17, listing element numbers. The fine mesh has 224 elements and 1095 nodes and is illustrated in Figure 10 on page 18. The weld area is shown in Figure 11 on page 19.

The same boundary conditions stated in [Ref. 1: p. 30] were applied. The right hand side of the model was fixed as illustrated in Figure 12 on page 20. A frictional surface was applied between the tube and the header. The nodes on the boundary were constrained together in the y direction but allowed to move with respect to each other in the z direction. This is in effect applying a contact surface with the coefficient of friction equal to zero.

### B. LOAD CONDITIONS

The same load conditions were applied as developed in [Ref. 1: pp. 38-42].

#### 1. Load condition no. 1 - Internal pressure load

Load condition no. 1 consisted of an internal pressure of 700 psi applied at all nodes located on the inside of the tube and header. This corresponds to the full rating of the boiler. This loading is illustrated in Figure 13 on page 21.

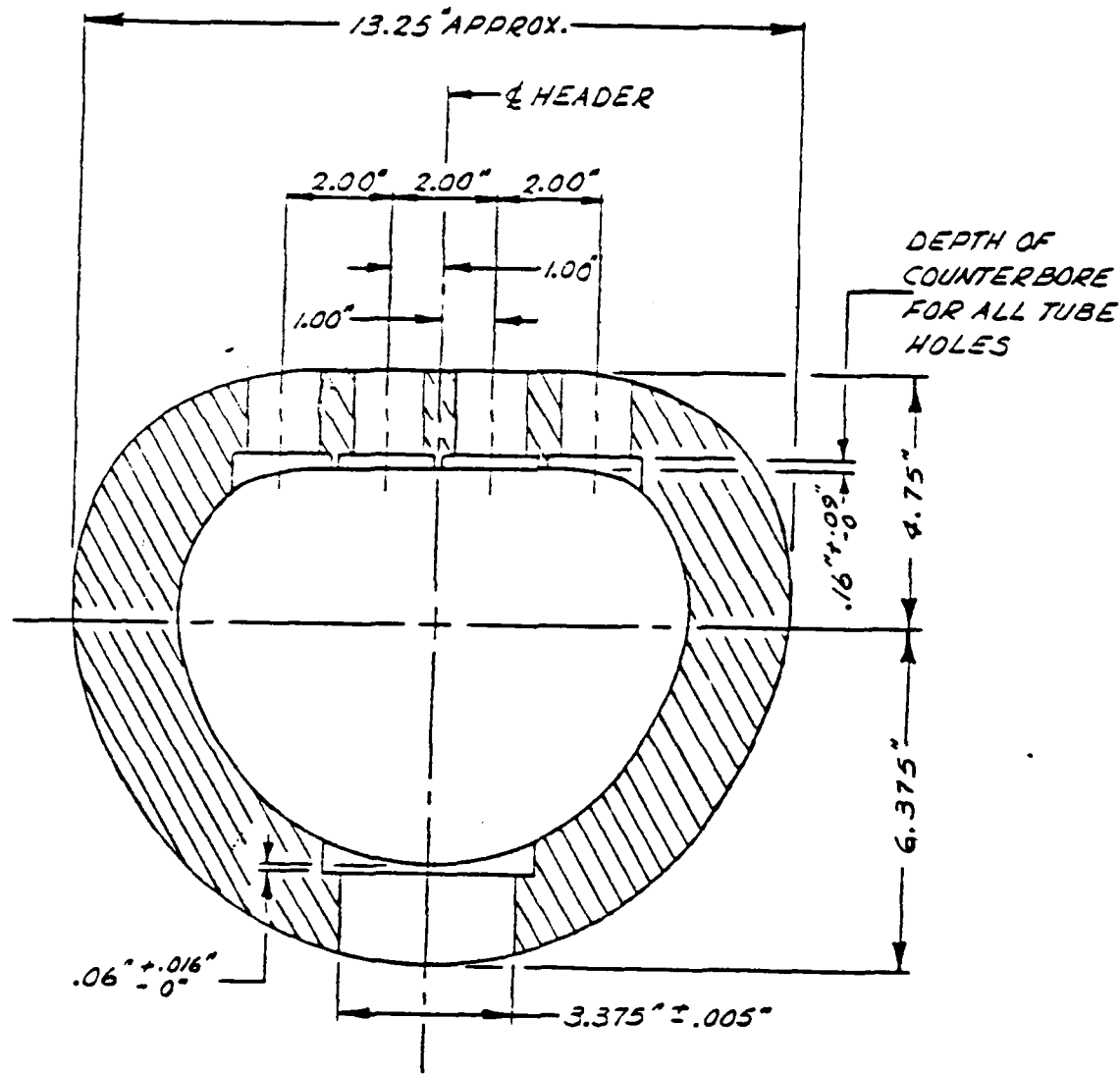
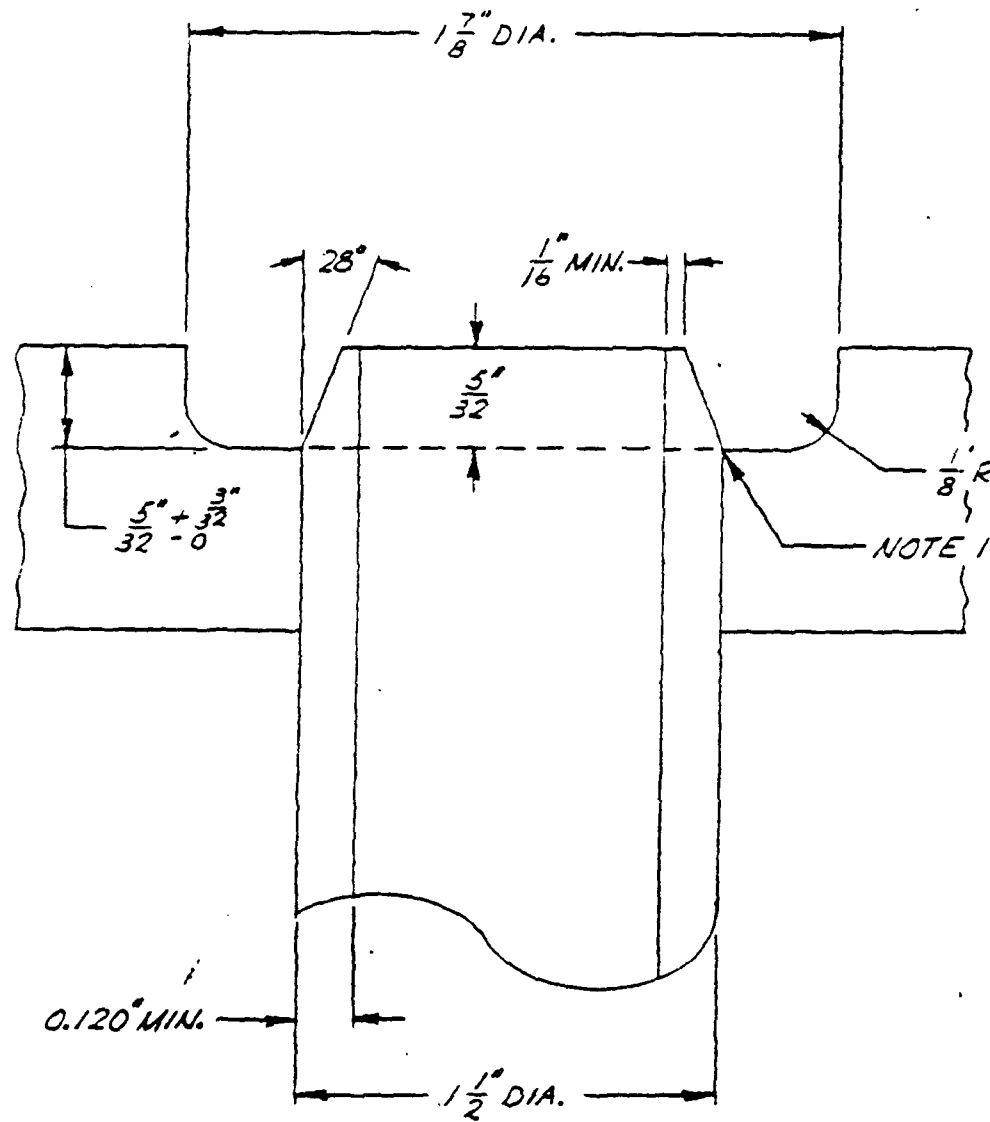


Figure 5. Cross sectional view of the superheater header



NOTE:

1. TUBE IS POSITIONED SUCH THAT BASE OF TUBE CHAMFER IS FLUSH WITH SQUARE CORNER AT BOTTOM OF COUNTERBORE AS SHOWN

Figure 6. Detail of the attachment weld joint

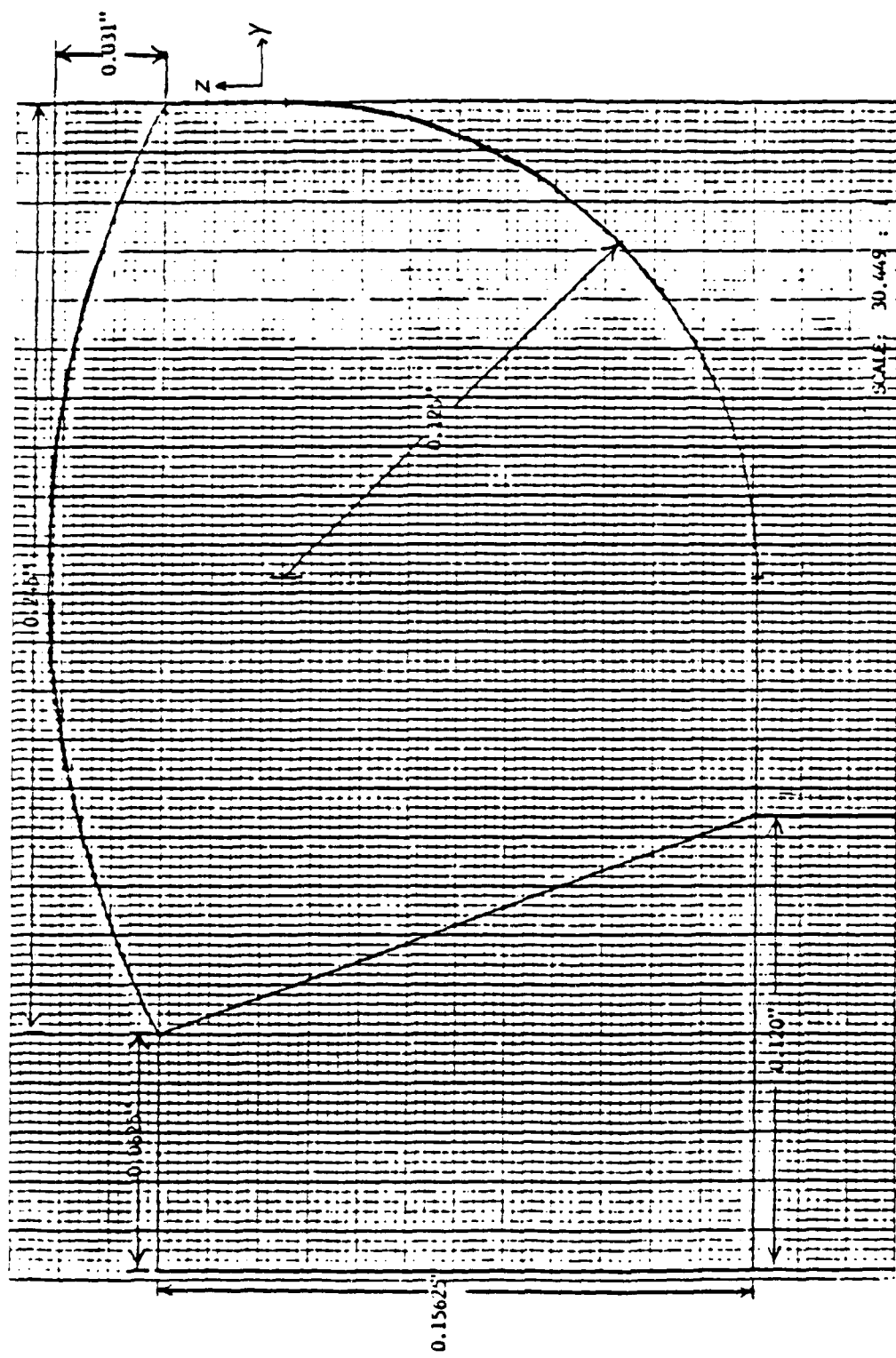


Figure 7. Geometry of the weld

HEADER  
ORIGINAL — D.262

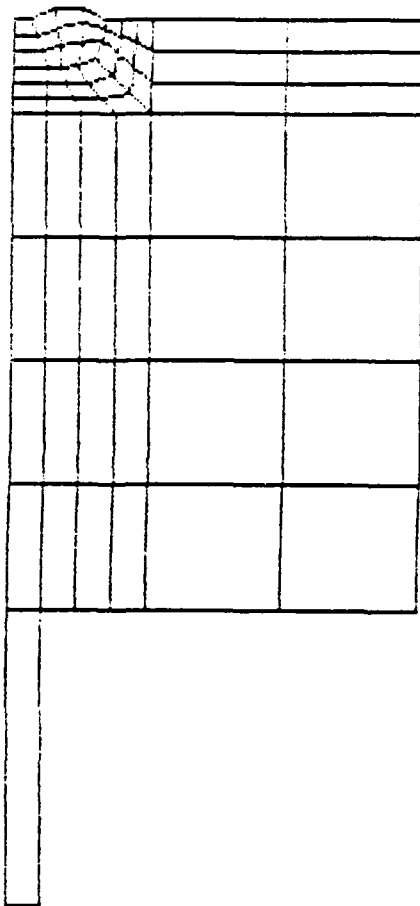


Figure 8. Coarse mesh

HEADER  
ORIGINAL → D.0170

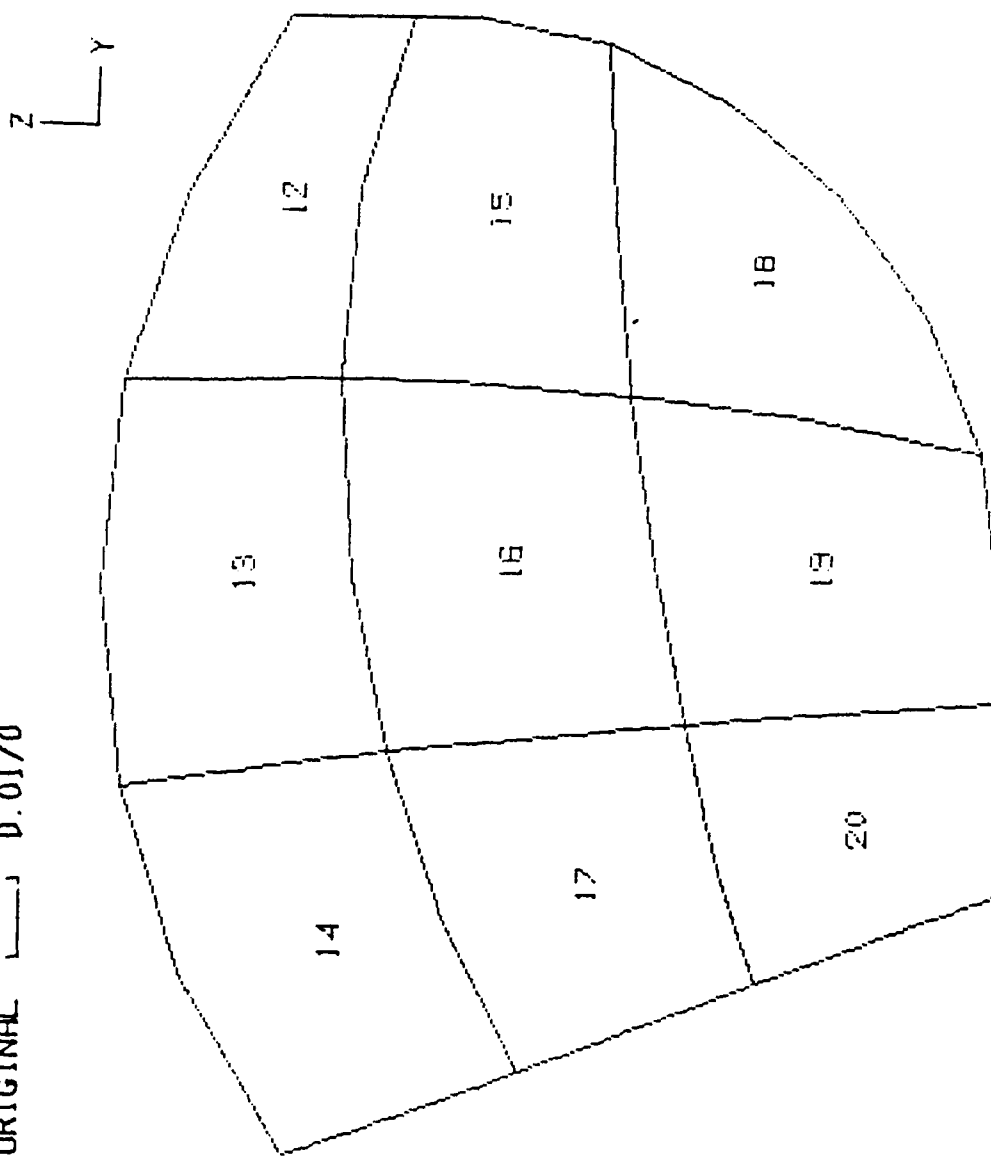


Figure 9. Close-up of the weld area, coarse mesh

HEADER

ORIGINAL D.262

Z

Y

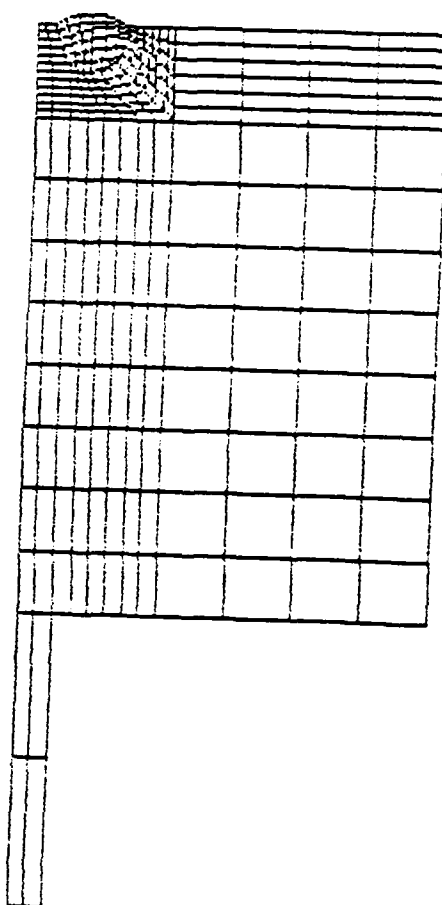


Figure 10. Fine mesh

HEADER  
ORIGINAL → D.0170

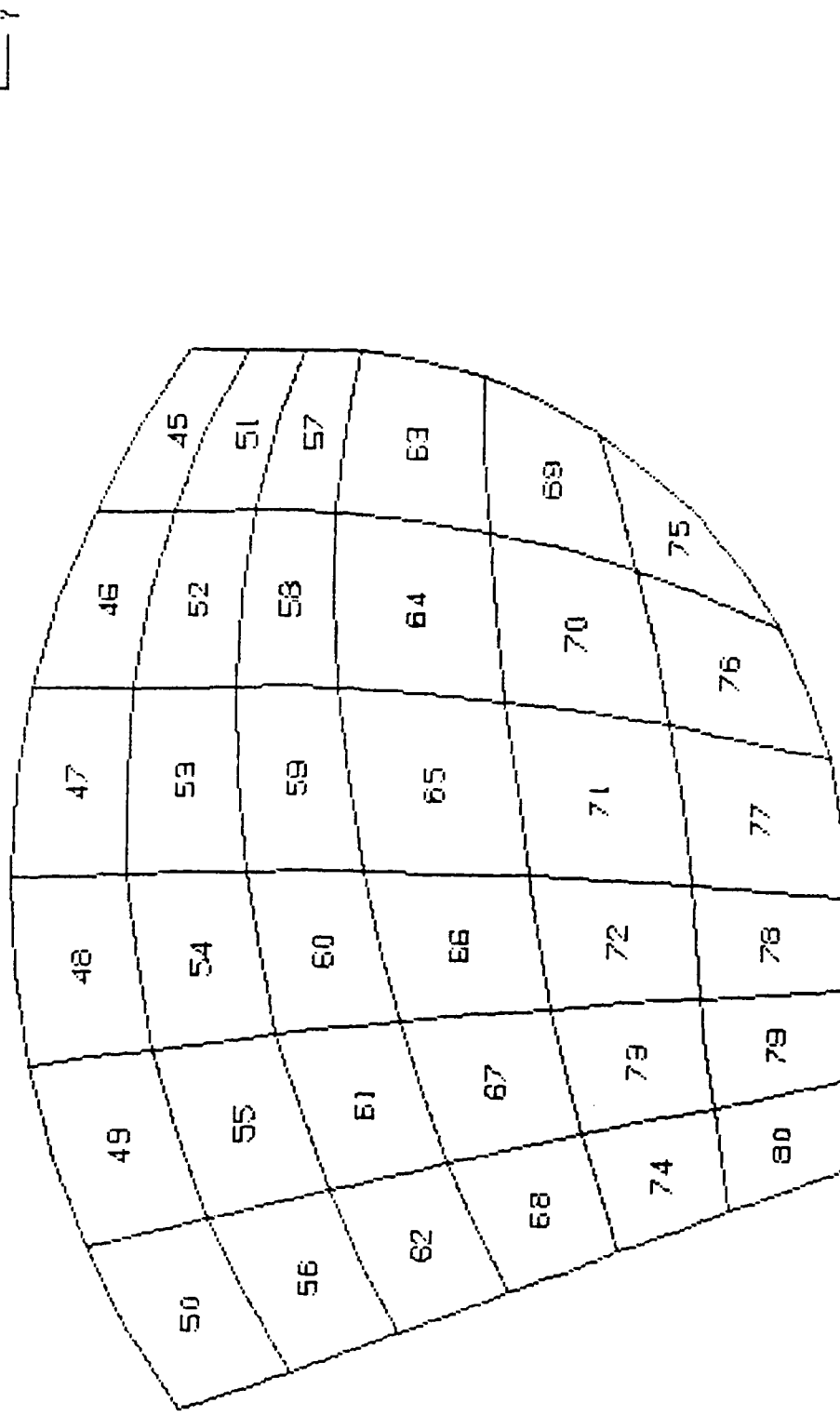


Figure 11. Close-up of the weld area, fine mesh

HEADER

ORIGINAL D.262

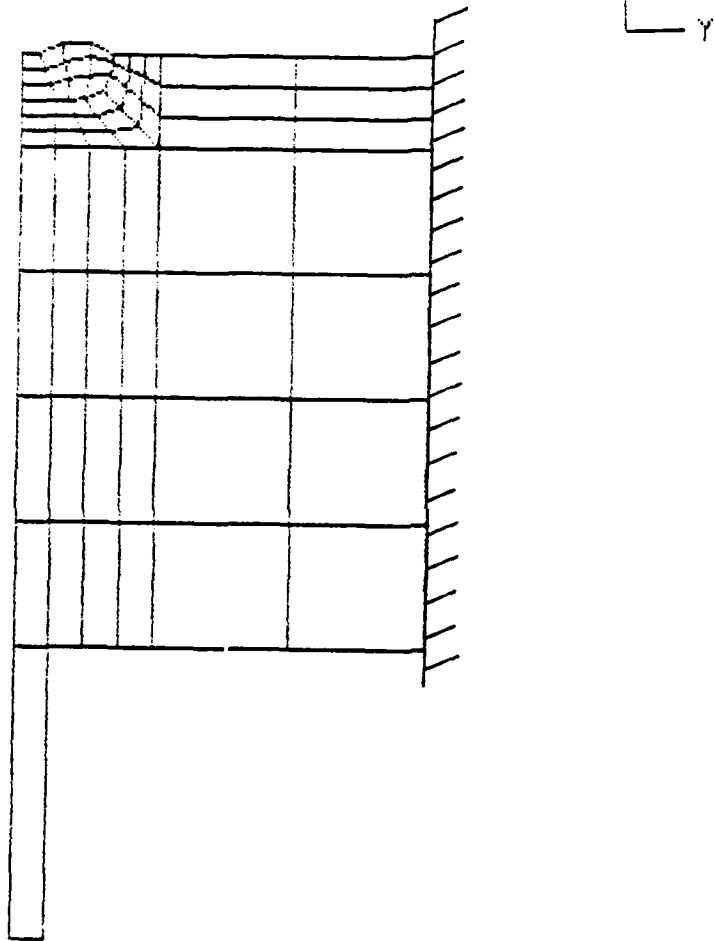


Figure 12. Fixed boundary conditions

HEADER  
ORIGINAL D. 262

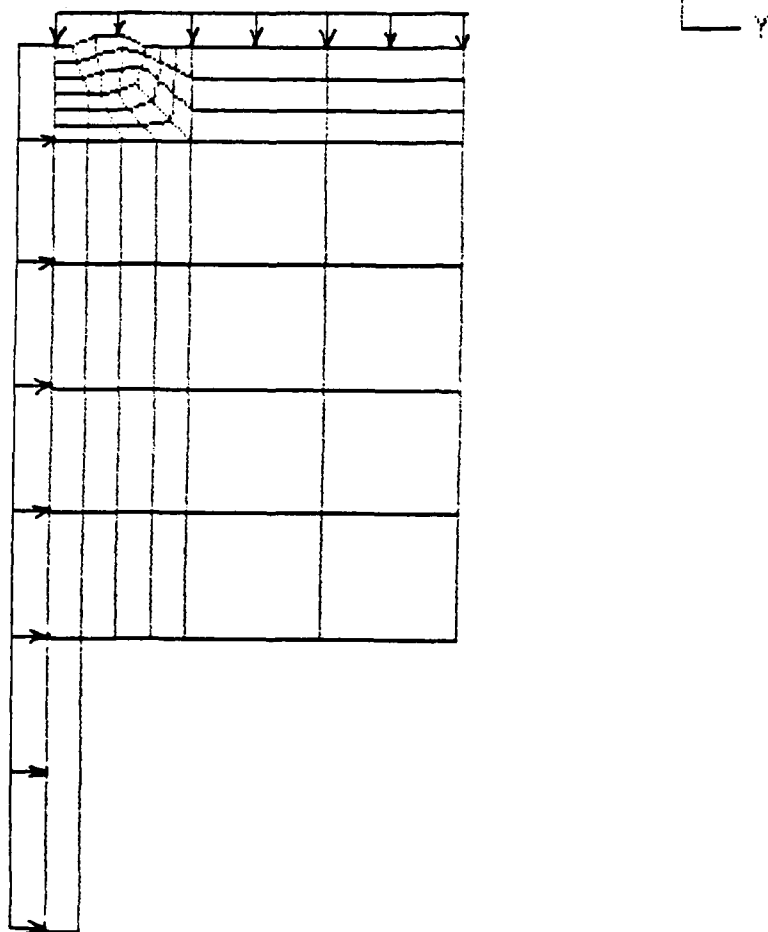


Figure 13. Load condition no. 1

## 2. Load condition no. 2 - Longitudinal tube load

The force per radian is 152 lbf. The coarse model uses the same consistent loading as [Ref. 1: p. 40]. The load was applied to the bottom element of the tube, on nodes 85, 68 and 87 as indicated in the following list:

- $F_{85} = F' (1/6) = 25.3 \text{ (Lb}_f\text{)}$
- $F_{68} = F' (2/3) = 101.3 \text{ (Lb}_f\text{)}$
- $F_{87} = F' (1/6) = 25.3 \text{ (Lb}_f\text{)}$

This is illustrated in Figure 14 on page 23. The consistent loading for the fine mesh was applied to nodes 85, 240, 239, 238 and 87 as follows:

- $F_{85} = F' (1/12) = 12.66666666 \text{ (Lb}_f\text{)}$
- $F_{240} = F' (1/3) = 50.66666666 \text{ (Lb}_f\text{)}$
- $F_{239} = F' (1/6) = 25.33333333 \text{ (Lb}_f\text{)}$
- $F_{238} = F' (1/3) = 50.66666666 \text{ (Lb}_f\text{)}$
- $F_{87} = F' (1/12) = 12.66666666 \text{ (Lb}_f\text{)}$

The consistent loading for the fine mesh is illustrated in Figure 15 on page 24.

## 3. Load condition no. 3 - Thermal load

The thermal load consists of maintaining a constant temperature of 350 degrees F at the interior nodes of the tube and header. A temperature gradient of 100 degrees F is applied to the right hand side of the model. This load condition is shown in Figure 16 on page 25.

## C. MATERIAL PROPERTIES

The same material properties were used as listed in [Ref. 1: p. 38]. Young's Modulus (E) equals 29,600,000 psi, the coefficient of thermal expansion ( $\alpha$ ) equals .0000065 in./in./°F and Poisson's ratio ( $\nu$ ) equals .3. The material of the tube and header is 2.25% chromium, 1% molybdenum steel (ASTM grade 22). The weld was assumed to have the same properties as the tube and header.

## D. COMPARISON OF RESULTS

The original and deformed shapes for load conditions 1, 2 and 3 for the coarse mesh are shown in Figure 17 on page 26, Figure 18 on page 27, and Figure 19 on page 28. The results for the fine mesh are shown in Figure 20 on page 29, Figure 21 on page 30, and Figure 22 on page 31. The maximum stresses in the weld for the coarse and fine

HEADER

ORIGINAL    D.0862

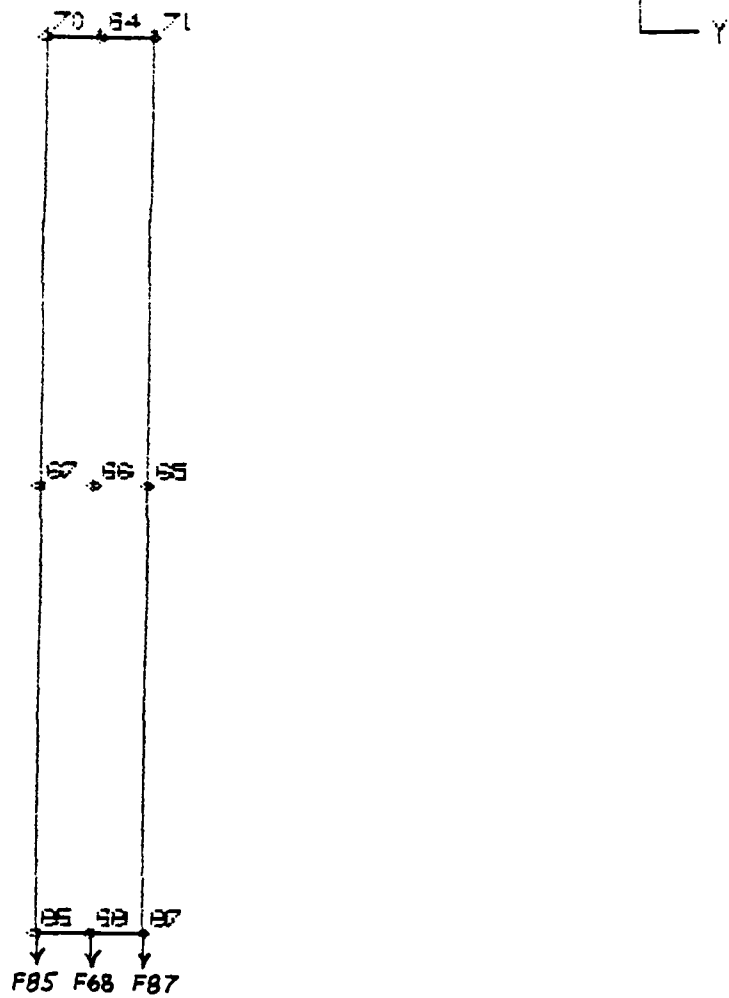


Figure 14. Load condition no. 2, coarse mesh

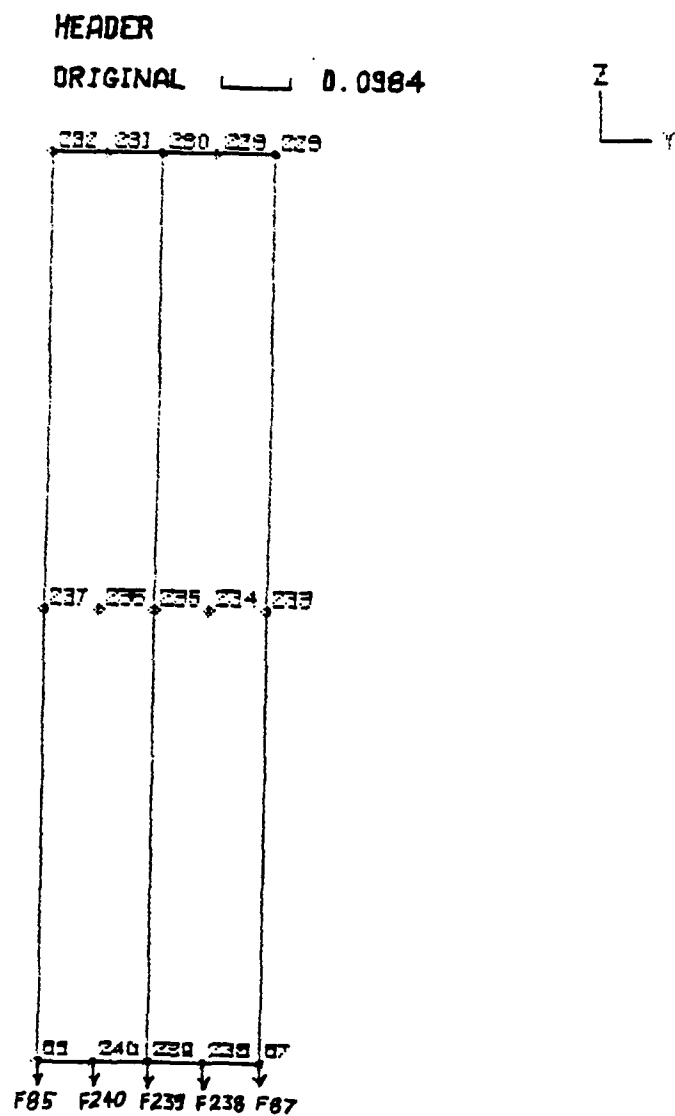


Figure 15. Load condition no. 2, fine mesh

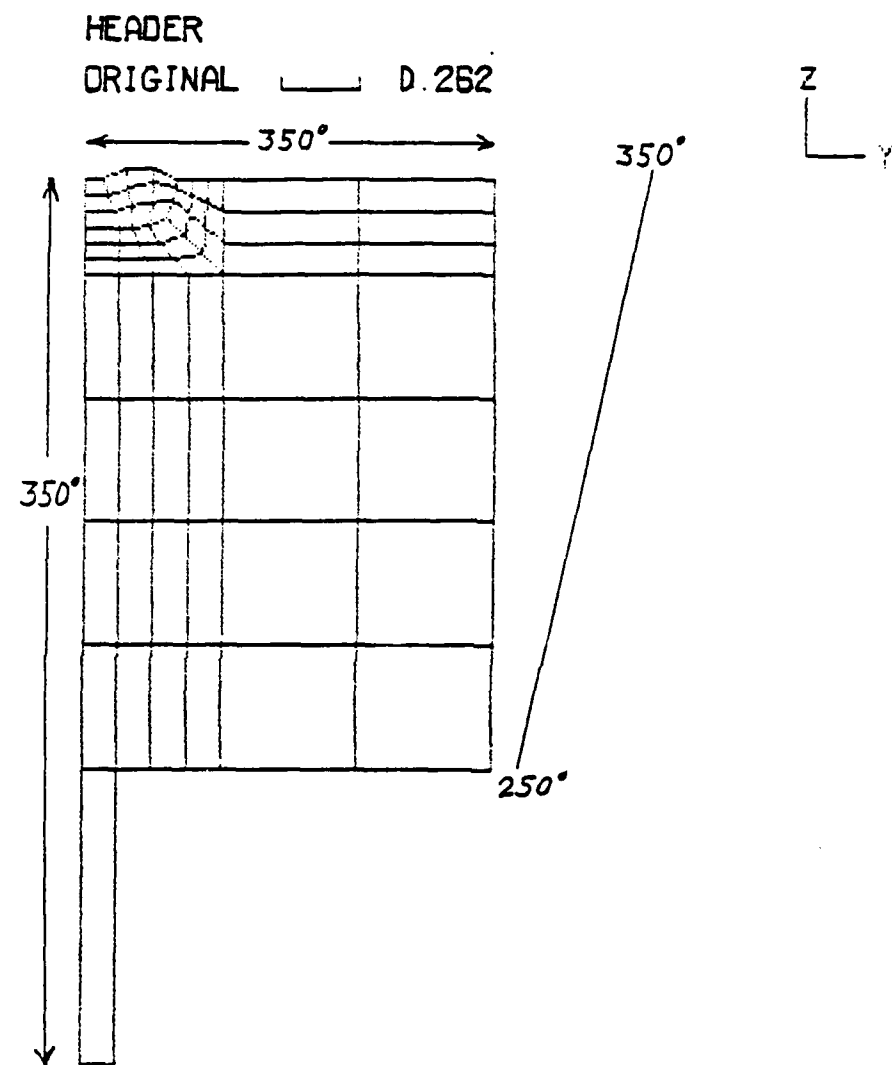


Figure 16. Load condition no. 3

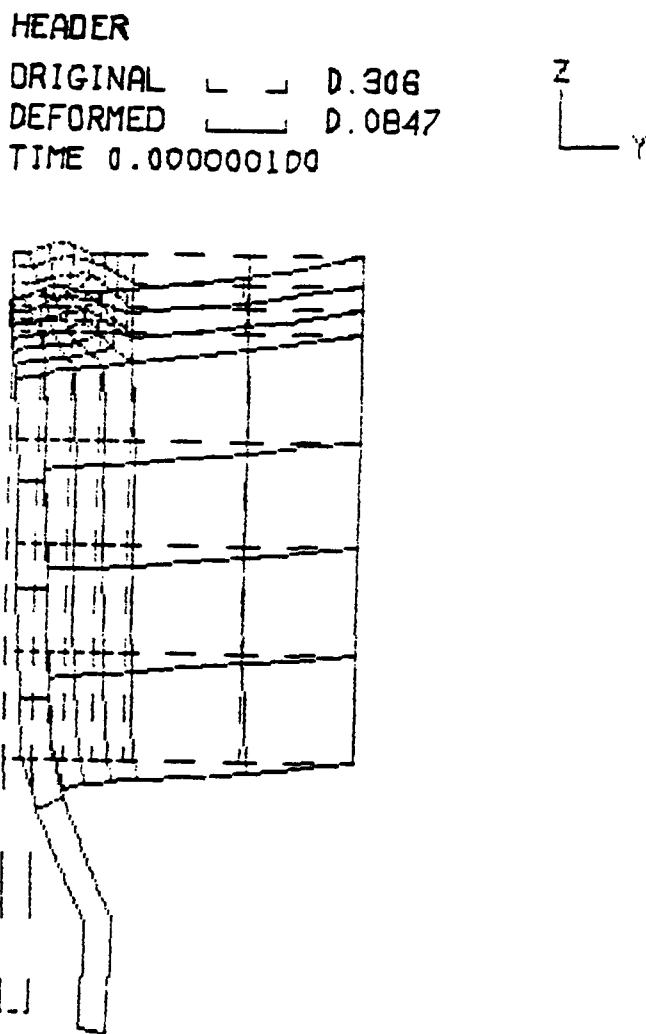


Figure 17. Original and deformed shape of coarse mesh for load condition no. 1

HEADER

ORIGINAL L - D.319  
DEFORMED L D.172  
TIME 0.000000100

Z  
Y

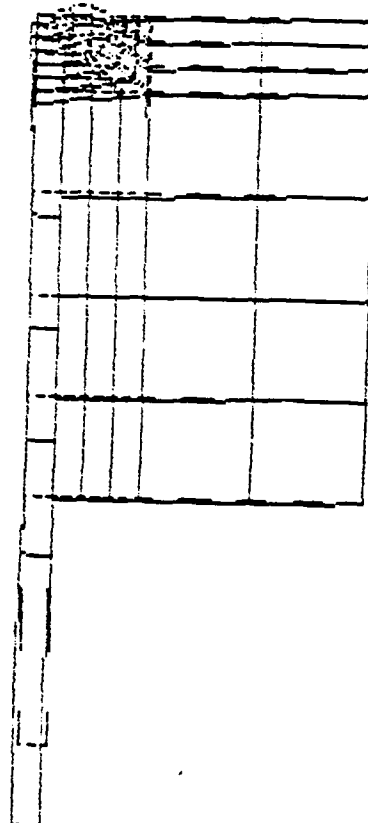


Figure 18. Original and deformed shape of coarse mesh for load condition no. 2

HEADER

ORIGINAL L L D.343  
DEFORMED L D.00606  
TIME 0.00000100

Z  
Y

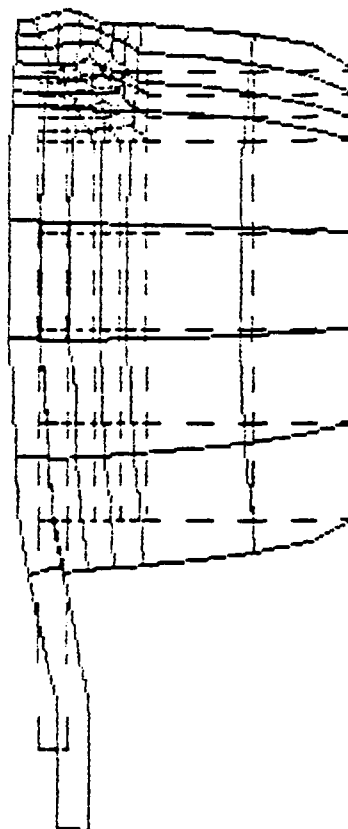


Figure 19. Original and deformed shape of coarse mesh for load condition no. 3

HEADER

ORIGINAL [ ] D.306  
DEFORMED [ ] D.0000871  
TIME 2.000

Z  
Y

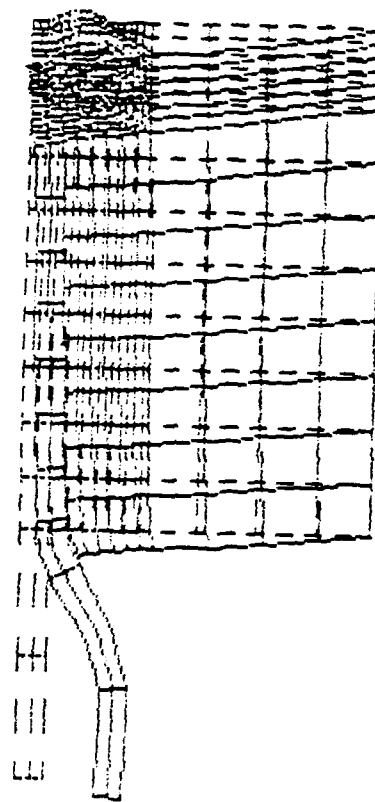


Figure 20. Original and deformed shape of fine mesh for load condition no. 1

HEADER

ORIGINAL    D.319  
DEFORMED    D.000174  
TIME 2.000

Z  
Y

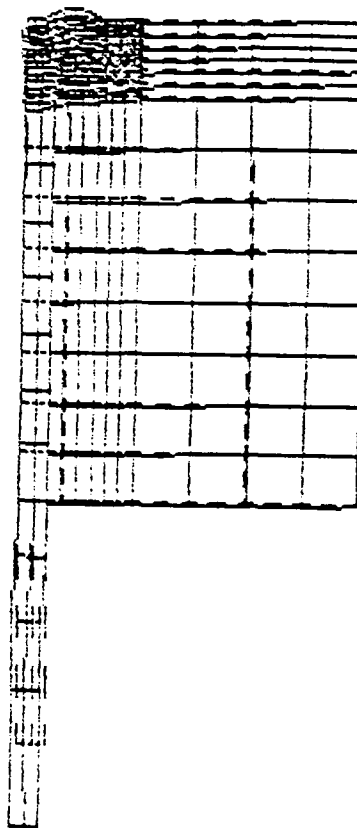


Figure 21. Original and deformed shape of fine mesh for load condition no. 2

HEADER

ORIGINAL    D.344  
DEFORMED    D.00590  
TIME 2.000

Z  
Y

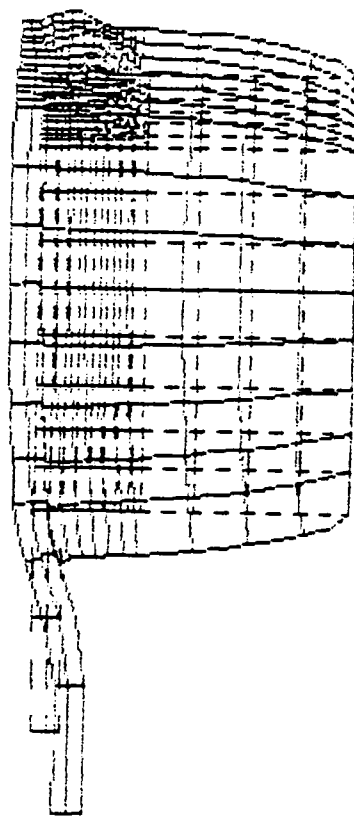


Figure 22. Original and deformed shape of fine mesh for load condition no. 3

mesh are listed in Table 1 and Table 2. For the axisymmetric problem,  $\sigma_{zz}$  is the hoop stress,  $\sigma_{rr}$  is the radial stress, and  $\sigma_{\theta\theta}$  is the longitudinal stress.

Table 1. MAXIMUM STRESSES FOR THE COARSE MESH

Stresses	Load Condition No. 1	Load Condition No. 2	Load Condition No. 3
$\sigma_{zz}$ (psi)	-636767E+03	-509766E+03	-135183E+06
$\sigma_{rr}$ (psi)	-661331E+03	-370531E+03	-466026E+05
$\sigma_{\theta\theta}$ (psi)	-742839E+03	-116857E+03	-559437E+04
$\sigma_{rz}$ (psi)	.120933E+03	.332004E+03	.134600E+05

Table 2. MAXIMUM STRESSES FOR THE FINE MESH

Stresses	Load Condition No. 1	Load Condition No. 2	Load Condition No. 3
$\sigma_{zz}$ (psi)	-649740E+03	-534142E+03	-136960E+06
$\sigma_{rr}$ (psi)	-659697E+03	.503587E+03	-555045E+05
$\sigma_{\theta\theta}$ (psi)	-753965E-03	-145094E+03	-980113E+04
$\sigma_{rz}$ (psi)	.136475E-03	.372948E+03	.193084E+05

The magnitude and direction of the principal stresses for the coarse and fine mesh, in the area of the weld, are listed in Table 3 and Table 4. A vector plot of the principal stresses of the coarse and fine mesh for load condition no. 3 is shown in Figure 23 on page 34 and Figure 24 on page 35.

Table 3. PRINCIPAL STRESSES FOR THE COARSE MESH

Element	P1 (psi)	P2 (psi)	Angle ( $^{\circ}F$ )
12	-1594E+03	-3422E+05	74.57
13	0.1352E+04	-1820E+05	85.39
14	0.2802E+03	-1413E+05	94.46
15	0.9153E+03	-3779E+05	86.39
16	0.3717E+04	-2807E+05	86.38
17	0.2304E+04	-2084E+05	86.18
18	0.1716E+04	-3808E+05	88.03
19	0.6323E+04	-3259E+05	87.72
20	0.3103E+04	-2530E+05	86.98

**Table 4. PRINCIPAL STRESSES FOR THE FINE MESH**

Element	P1 (psi)	P2 (psi)	Angle ( $^{\circ}$ F)
45	.8641E+03	.4057E+05	67.64
46	.8286E+03	.2143E+05	73.66
47	.8814E+03	.1572E+05	82
48	.6244E+03	.1315E+05	90.31
49	.2067E+03	.1219E+05	98.49
50	.5970E+03	.1293E+05	103.33
51	.1553E+04	.4200E+05	80.67
52	.2516E+04	.3006E+05	79.02
53	.2590E+04	.2272E+05	82.48
54	.2192E+04	.1923E+05	86.37
55	.1592E+04	.1725E+05	89.20
56	.2959E+03	.1531E+05	88.85
57	.2147E+04	.4153E+05	85.36
58	.2898E+04	.3440E+05	84.10
59	.3626E+04	.2802E+05	84.60
60	.3324E+04	.2402E+05	85.88
61	.2581E+04	.2107E+05	86.41
62	.1310E+04	.1789E+05	86.05
63	.1468E+04	.2044E+05	87.31
64	.2494E+04	.3631E+05	87.32
65	.3856E+04	.3161E+05	86.70
66	.3772E+04	.2755E+05	86.46
67	.2107E+04	.2403E+05	86.19
68	.2107E+04	.2036E+05	85.89
69	.1507E+02	.3976E+05	87.96
70	.2439E+04	.3685E+05	88.22
71	.3705E+04	.3322E+05	87.71
72	.3793E+04	.2956E+05	87.17
73	.3364E+04	.2615E+05	86.76
74	.2660E+04	.2252E+05	86.44
75	.1317E+04	.3915E+05	88.01
76	.2801E+04	.3685E+05	88.09
77	.3636E+04	.3375E+05	97.90
78	.3742E+04	.3055E+05	87.62
79	.3503E+04	.2759E+05	87.37
80	.3035E+04	.2437E+05	87.13

The maximum hoop stress listed in [Ref. 1: pp. 39-40] for load condition no. 1 is .69 (ksi) and the maximum hoop stress for load condition no. 2 is .96 (ksi). Those results compare favorably with the results shown here from ADINA. [Ref. 1: p. 42] indicates the maximum hoop stress for load condition no. 3 is 19.0 (ksi). This value is much smaller than the result of 137 (ksi) obtained with ADINA. In considering the verification of ADINA as explained in chapter three, it is believed that the results obtained here are correct. The results confirm that the thermal stresses are the predominant stresses.

HEADER

DEFORMED 0.0189  
TIME 0.00000100

X  
Y

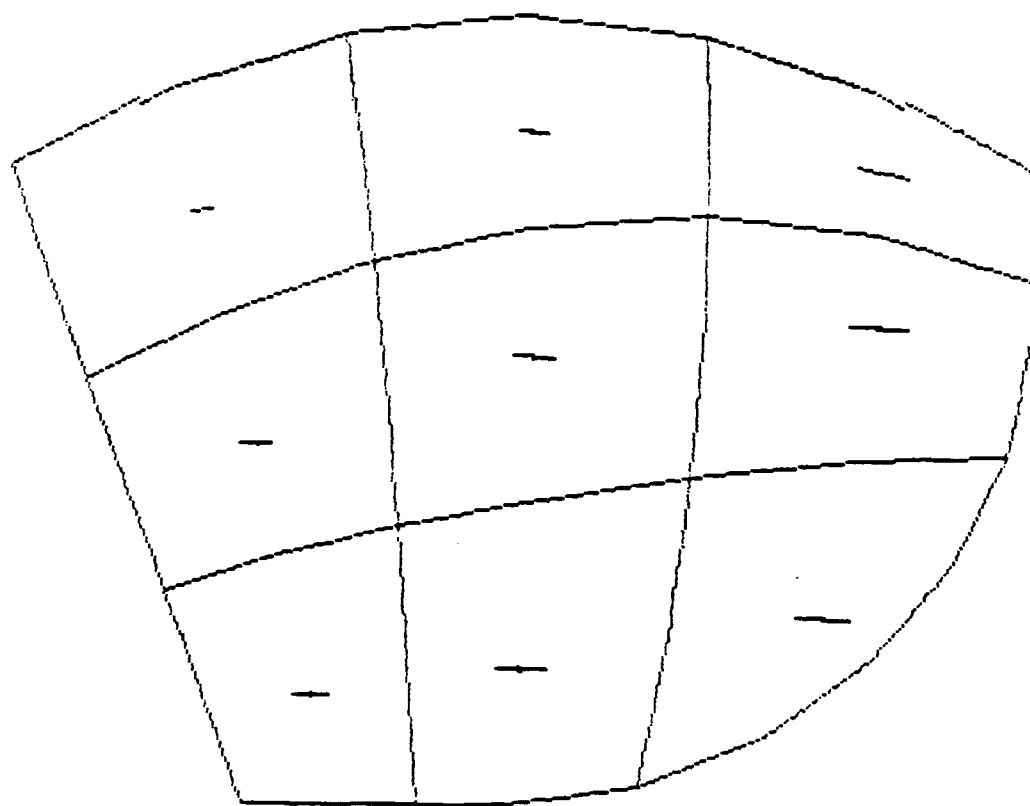


Figure 23. Vector plot of the principal stresses of the coarse mesh for load condition no. 3

HEADER

DEFORMED D.0189  
TIME 2.000

Z  
Y

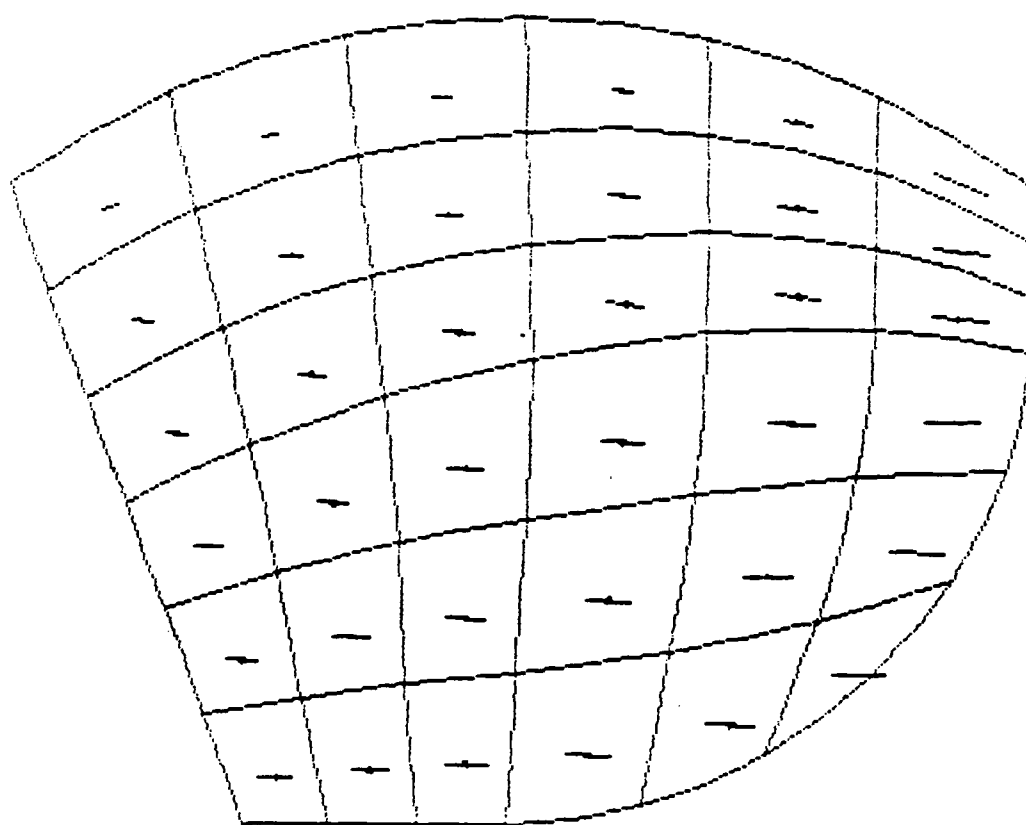


Figure 24. Vector plot of the principal stresses of the fine mesh for load condition no. 3

The accuracy of the results of the problem that has been modeled are very good. There is very little difference between the results of the coarse and fine mesh which means convergence has been achieved. There is no significant difference in the calculated stresses at the boundaries of adjacent elements.

The next step was to use the contact surface option of ADINA for the boundary between the tube and the header. This allows an indication of the coefficient of friction and a determination of its effect on the solution. The maximum stresses are shown in Table 5 and Table 6 for the coarse and fine mesh for a coefficient of friction of zero. These results compare very well with the previous results.

Table 5. MAXIMUM STRESSES FOR THE COARSE MESH, CONTACT SURFACE OPTION

Stresses	Load Condition No. 1	Load Condition No. 2	Load Condition No. 3
$\sigma_{xx}$ (psi)	-.646923E+03	-.514228E+03	-.135265E+06
$\sigma_{yy}$ (psi)	-.657614E+03	.362559E+03	-.465231E+05
$\sigma_{zz}$ (psi)	-.747963E+03	-.112506E+03	-.558613E+04
$\sigma_{vz}$ (psi)	.134382E+03	.328554E+03	.134376E+05

Table 6. MAXIMUM STRESSES FOR THE FINE MESH, CONTACT SURFACE OPTION

Stresses	Load Condition No. 1	Load Condition No. 2	Load Condition No. 3
$\sigma_{xx}$ (psi)	-.646745E+03	-.537235E+03	-.137053E+06
$\sigma_{yy}$ (psi)	-.657250E+03	.495395E+03	-.553930E+05
$\sigma_{zz}$ (psi)	-.757047E+03	-.139909E+03	-.978366E+04
$\sigma_{vz}$ (psi)	.139310E+03	.366954E+03	.192709E+05

## E. FURTHER MODEL DEVELOPMENT

A detailed study of the problem and the results obtained in the previous section indicated some changes were needed in the model.

It was discovered that the model as developed was not a repeating section. The distance between the center of the tubes is two inches. The right hand side of the model is two inches from the center of the tube. A new model was developed with the right hand side being one inch from the center of the tube. The coarse mesh consists of 43

elements and 211 nodes. The fine mesh has 172 elements and 763 nodes. The models are shown in Figure 25 on page 38 and Figure 26 on page 39.

Figure 19 on page 28 and Figure 22 on page 31 prompted a change in boundary conditions. The deformed shapes showed that the header was not allowed to expand uniformly in the axial direction. The bottom node of the right hand side of the header was fixed and the rest of the nodes on the right hand side were allowed to roll in the z direction. These boundary conditions are shown in Figure 27 on page 40.

The original and deformed shapes for load conditions 1, 2 and 3 for the coarse mesh are shown in Figure 28 on page 41, Figure 29 on page 42 and Figure 30 on page 43. Figure 30 on page 43 shows that the header is now expanding uniformly in the axial direction. The maximum stresses are indicated in Table 7 and Table 8 for the coarse and fine mesh. The ADINA-IN input file for these models is listed in Appendix G.

Table 7. MAXIMUM STRESSES FOR THE COARSE MESH, REPEATING SECTION

Stresses	Load Condition No. 1	Load Conditions 1 and 2	Load Condition No. 3
$\sigma_{xx}$ (psi)	-.420381E+03	-.566508E+03	-.997953E+05
$\sigma_{yy}$ (psi)	-.597283E+03	.792176E+03	-.373304E+05
$\sigma_{zz}$ (psi)	-.825134E+03	-.112852E+04	-.454326E+04
$\sigma_{yz}$ (psi)	.231712E+03	.838120E+03	.104692E+05

Table 8. MAXIMUM STRESSES FOR THE FINE MESH, REPEATING SECTION

Stresses	Load Condition No. 1	Load Conditions 1 and 2	Load Condition No. 3
$\sigma_{xx}$ (psi)	-.473741E+03	-.595979E+03	-.101403E+06
$\sigma_{yy}$ (psi)	-.840852E+03	.130359E+04	-.447373E+05
$\sigma_{zz}$ (psi)	-.922094E+03	-.126150E+04	-.796674E+04
$\sigma_{yz}$ (psi)	.313721E+03	.102645E+04	.151684E+05

#### F. THERMAL GRADIENTS.

The previous change in the model made the thermal gradient in the area of the weld very flat. It was desired to determine what effect different thermal gradients on the right

REPEAT HEADER  
ORIGINAL — D.262

Z  
Y

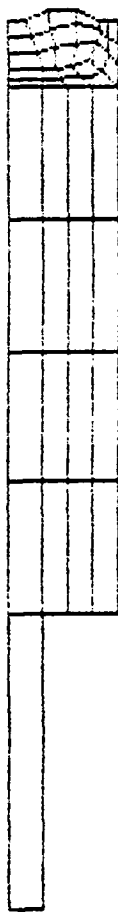


Figure 25. Coarse mesh, repeating section

HEADER  
ORIGINAL D.262

Z  
Y



Figure 26. Fine mesh, repeating section

REPEAT HEADER  
ORIGINAL D.262

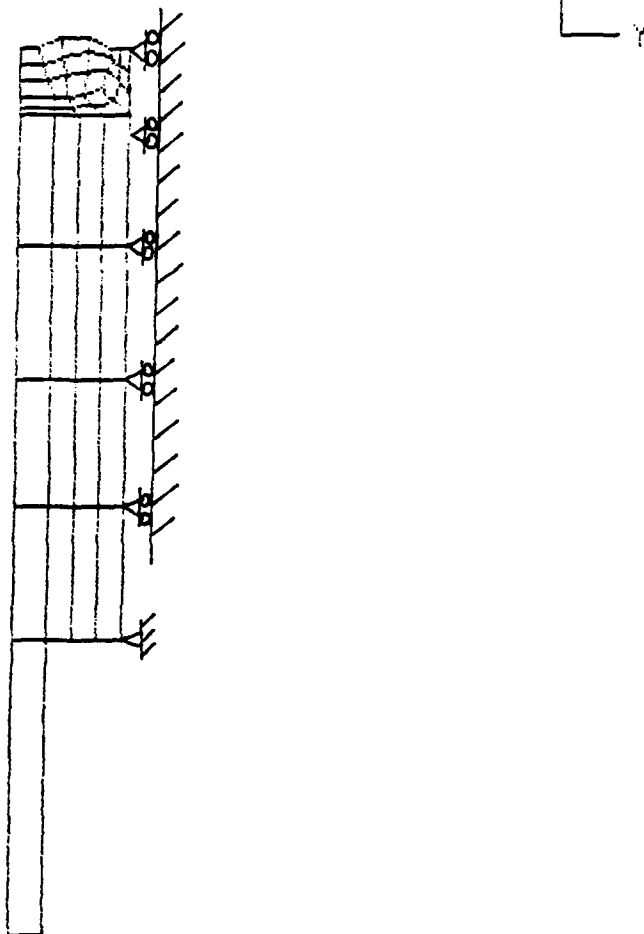


Figure 27. Rolling boundary conditions

REPEAT HEADER

ORIGINAL 0.315  
DEFORMED 0.0000847  
TIME 2.000

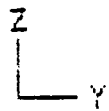


Figure 28. Original and deformed shape of coarse mesh for load condition no.1, repeating section

REPEAT HEADER

ORIGINAL    D.319  
DEFORMED    D.000250  
TIME 2.000

Z  
Y



Figure 29. Original and deformed shape of coarse mesh for load condition no. 2 ,  
repeating section

REPEAT HEADER

ORIGINAL [ ] 0.341  
DEFORMED [ ] 0.00559  
TIME 2.000

Z  
Y



Figure 30. Original and deformed shape of coarse mesh for load condition no. 3 ,  
repeating section

hand side of the model would have on the results. The maximum stresses for a thermal gradient of 100, 10, 2 and 0 degrees F are shown in Table 9.

Table 9. MAXIMUM STRESSES FOR DIFFERENT THERMAL GRADIENTS

Thermal Gradient	$\sigma_{xx}$ (psi)	$\sigma_{yy}$ (psi)	$\sigma_{zz}$ (psi)	$\sigma_{yz}$ (psi)
100° F	-.997953E+05	-.373304E+05	-.454326E+04	.104692E+05
10° F	-.998908E+05	-.373122E+05	-.454017E+04	.104358E+05
2° F	-.998993E+05	-.373106E+05	-.453990E+04	.104328E+05
0° F	-.999015E+05	-.373102E+05	-.453983E+04	.104321E+05

The results were surprising. The size of the gradient had very little effect on the magnitude of the stresses. The stresses remained very high even for a zero thermal gradient. A study of these results indicated the need for different boundary conditions. Restricting the right hand side of the model to move in the z direction only was not allowing the header to expand outwardly in the radial direction. The header was being forced to expand into the center of the tube which was creating the high stresses in the area of the weld.

The boundary condition chosen is shown in Figure 31 on page 45. The bottom left hand node of the header at the boundary of the tube and the header was fixed. The rest of the bottom nodes of the header were allowed to roll in the y direction. The contact surface option of ADINA could not be used for this solution. The nodes on the boundary were constrained together in the y direction and allowed to move with respect to one another in the z direction, modeling a contact surface with zero coefficient of friction. This was with the exception of the bottom left hand node of the header.

An iterative procedure was then followed to determine the solution of the problem. After each run of the problem, the bottom left hand node of the header was given a permanent displacement to the right equal to the displacement of the corresponding node of the tube at the boundary. This was continued until no overlap occurred. The original and deformed shapes of the final iteration for load condition no. 3 are shown in Figure 32 on page 46. As can be seen, the model is now expanding uniformly in the

REPEAT HEADER  
ORIGINAL D.262

Z  
V

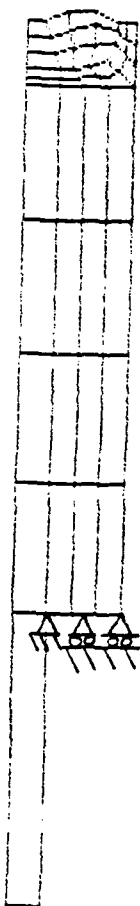


Figure 31. Bottom rolling boundary condition

REPEAT HEADER

ORIGINAL [ ] D. 349  
DEFORMED [ ] D. 00369  
TIME 2.000

Z  
Y

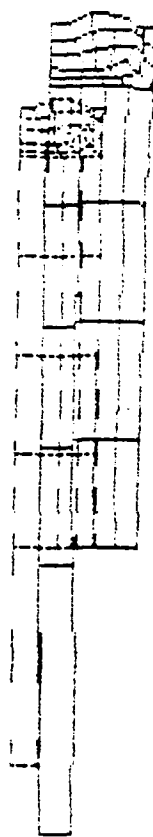


Figure 32. Original and deformed shape of the fine mesh for load condition no. 3, expanding radially and axially

axial direction and outwardly in the radial direction. The maximum stresses in the weld area of the coarse mesh for load condition no. 3 are shown in Table 10.

Table 10. MAXIMUM STRESSES FOR THE COARSE MESH, EXPANDING RADIALLY

Stresses	Load Condition No. 3
$\sigma_{xx}$ (psi)	.460123E+03
$\sigma_{yy}$ (psi)	-.932915E+02
$\sigma_{zz}$ (psi)	.102227E+03
$\sigma_{yz}$ (psi)	-.584215E+02

These results are much lower than those obtained for the previous model and it is believed that these results are closer to the actual stresses. However, it is also believed that this model is not a true repeating section in that the expansion of the neighboring tubes and the rest of the header will have an effect on this section, probably raising the stresses in the weld area. The need for a 3-dimensional model was indicated.

A 3-dimensional model was also desired in order to apply non-symmetric loading to the model. The major difference between this header and other headers with a similar cross section is that this header is not sectionalized. It has one inlet/outlet header and one intermediate header. This results in a larger temperature gradient from the inlet to the outlet side. A 3-dimensional model would allow this type of non-symmetric loading to be studied.

## V. 3-DIMENSIONAL SOLID FINITE ELEMENT MODEL

### A. MODEL DEVELOPMENT

The repeating section chosen to be modeled was one tube row. Only half of the row was modeled due to symmetry. The welds were assumed to have the same material properties as the tube and header and no attempt was made to substructure the weld area.

The element chosen to model the structure was the 20-node isoparametric solid element. This element is shown in Figure 33 on page 49.

Figure 34 on page 50 shows the modeling of one tube. Each tube consists of sixty elements. Figure 35 on page 51 shows how the header was connected to the tube. A contact surface was placed between the tube and the header. The entire model is shown in Figure 36 on page 52. Figure 37 on page 53 is another view of the model showing the location of the origin of the axis. The model consists of 288 elements and 1957 nodes. Figure 38 on page 54, Figure 39 on page 55 and Figure 40 on page 56 show a view of the model looking from the x, y and z directions.

The hidden line computer code developed by David R. Hedgley, Jr. of the Ames Research Center was utilized to check the model. Different views are shown in Figure 41 on page 57 and Figure 42 on page 58.

The following boundary conditions were imposed. Every node in the  $y=0$  plane was constrained to roll in that plane. In addition the node at the origin was fixed and the nodes above the origin along the positive x axis were constrained to roll only in the x direction.

### B. INTERNAL PRESSURE LOAD

The internal pressure load of 700 psi was applied to the inside nodes of the tube and header. It was then discovered that ADINA does not optimize the band-width of contact surfaces. The bandwidth of this model is approximately 2700 and the problem was too large to be solved on the VAX/VMS operating system. The ADINA-IN input file for the contact surfaces is listed in Appendix II for reference.

A contact surface was then modeled by constraining the corresponding nodes of the tube and header to move together in the y and z direction, but allowing them to move relative to one another in the x direction. This assumes a coefficient of friction of zero and reduced the bandwidth to approximately 1000.

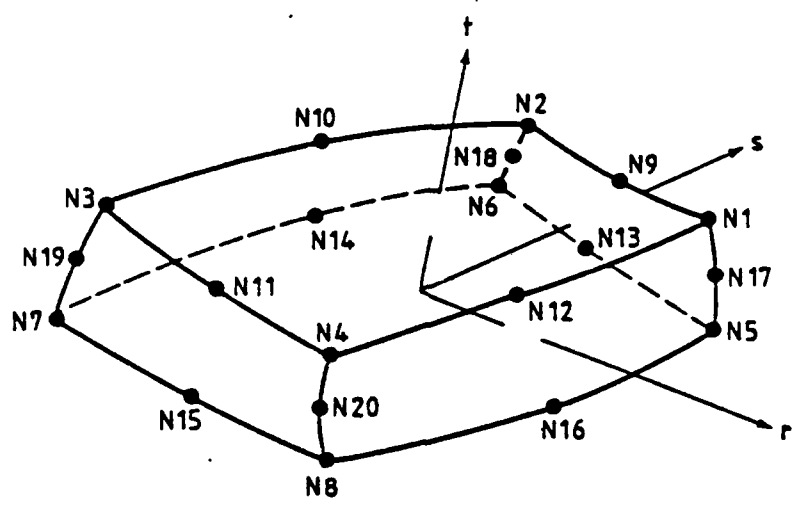


Figure 33. 20-node isoparametric solid element

3D-HEADER  
ORIGINAL — D.258

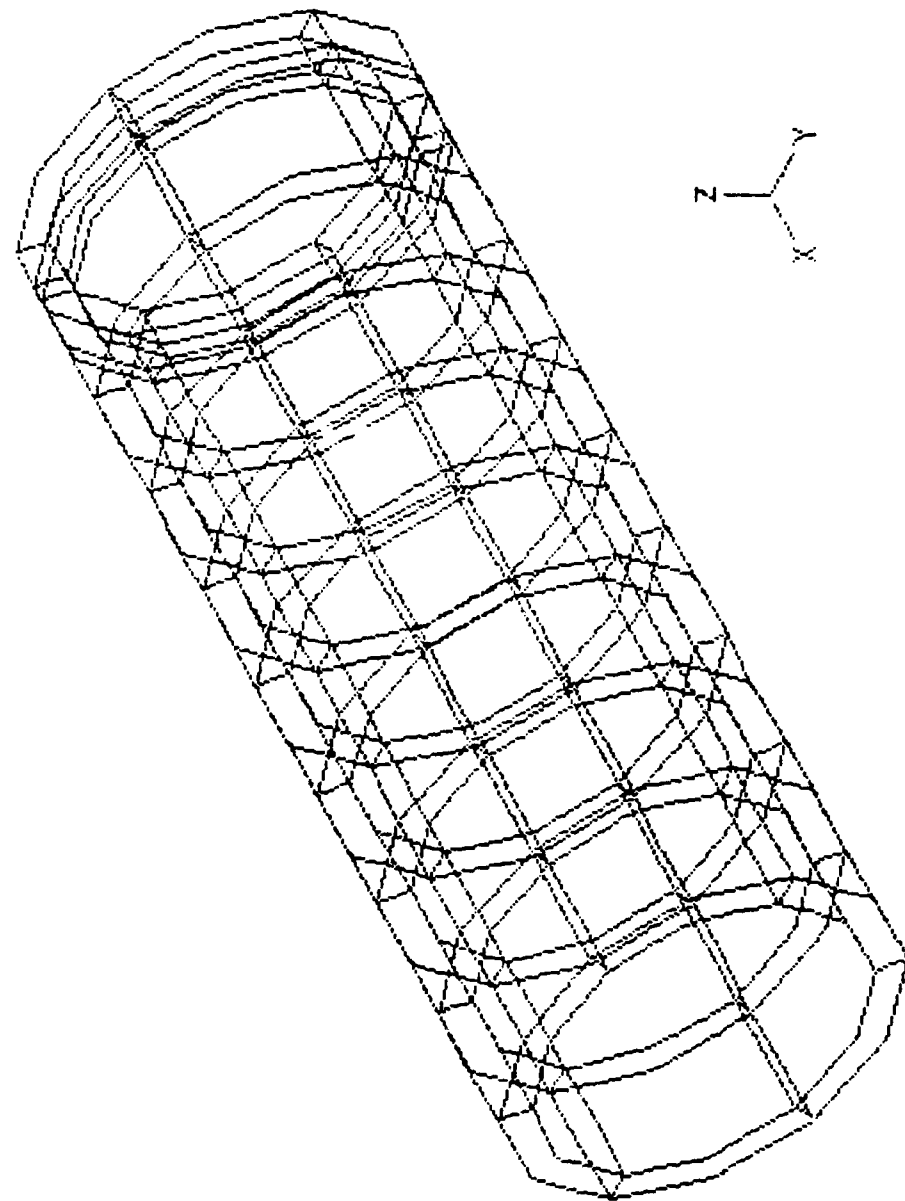


Figure 34. Mesh for one tube

3D-HEADER

ORIGINAL D. 194

Z  
Y

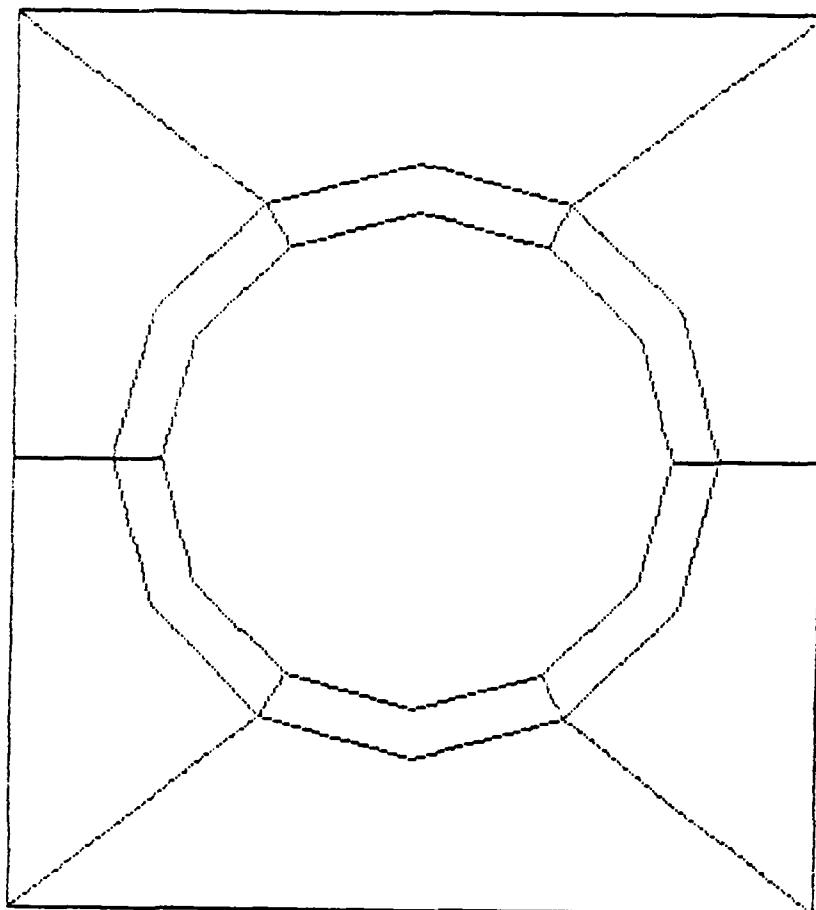


Figure 35. Attachment of header to a tube

3D-HEADER  
ORIGINAL — D.715

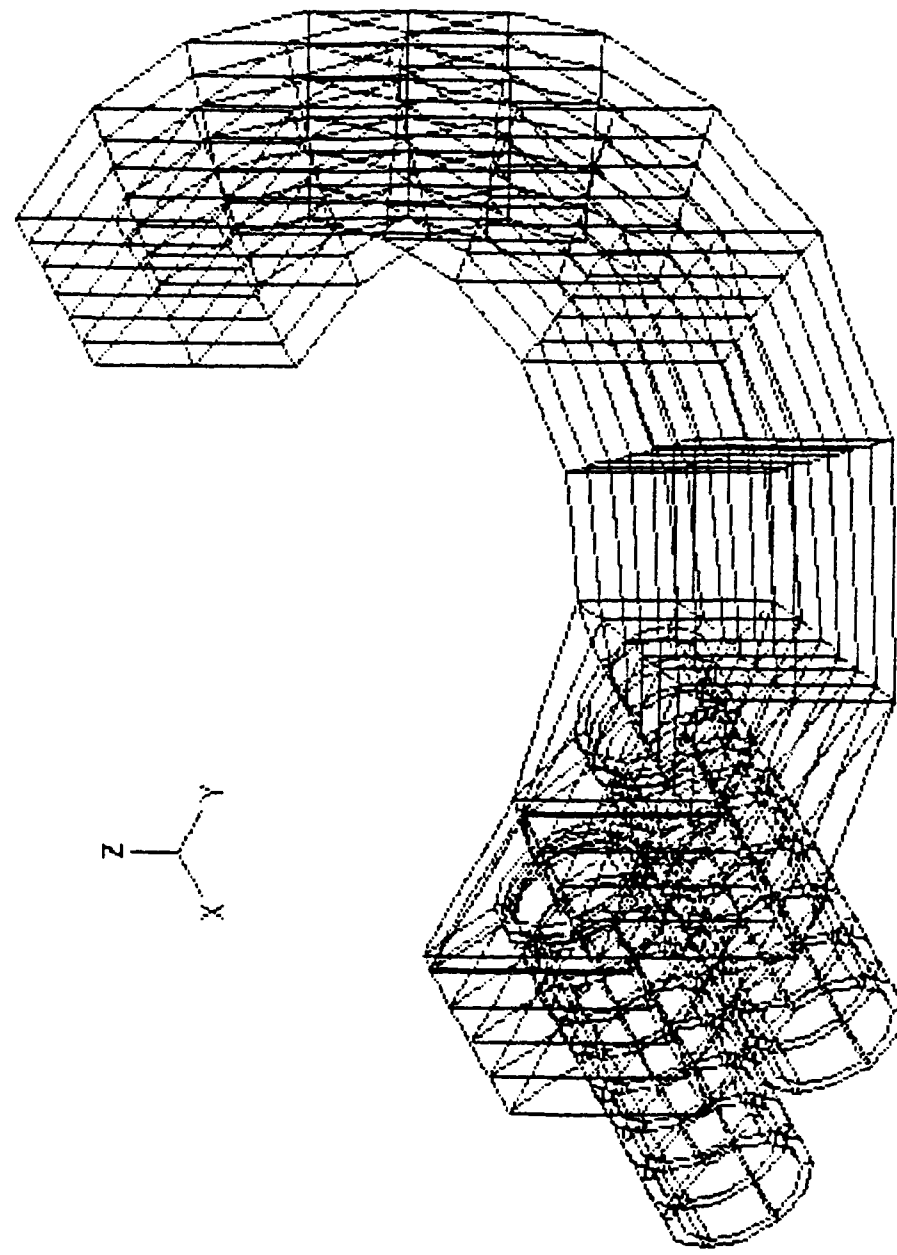


Figure 36. 3-dimensional model

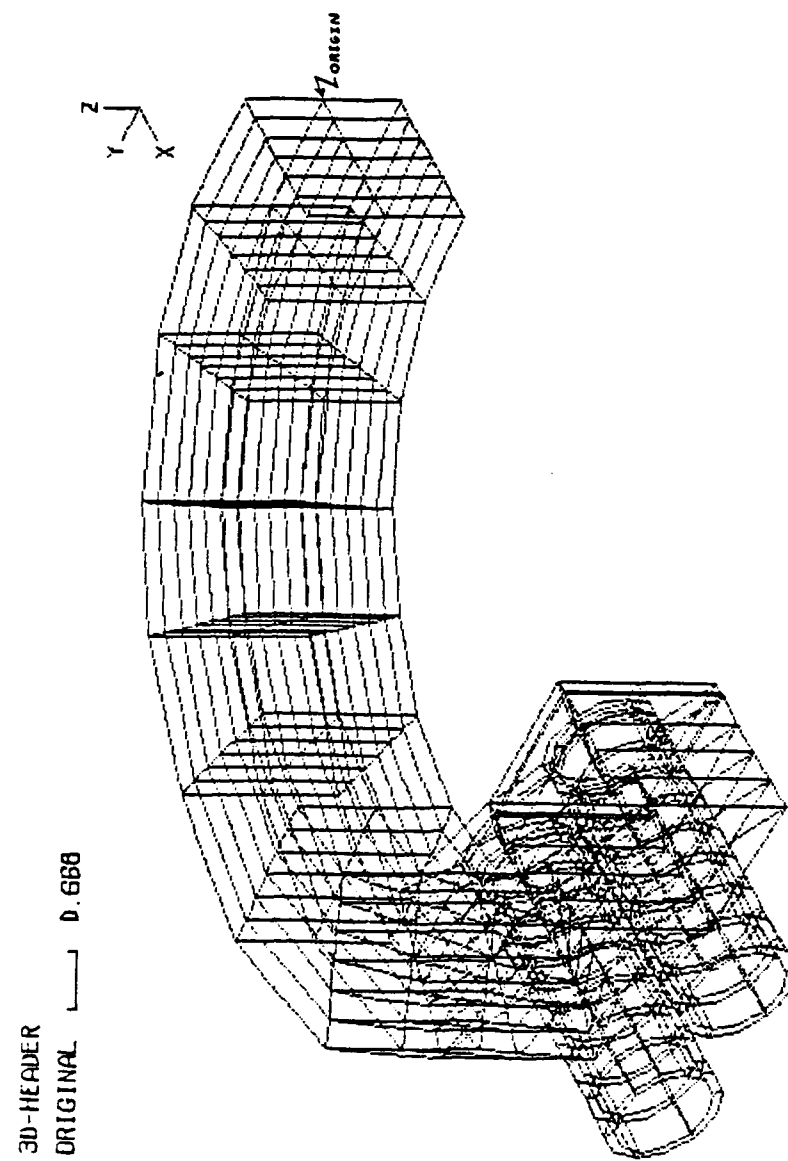


Figure 37. 3-dimensional model showing the location of the origin

3D-HEADER  
ORIGINAL → D. 956

z  
y

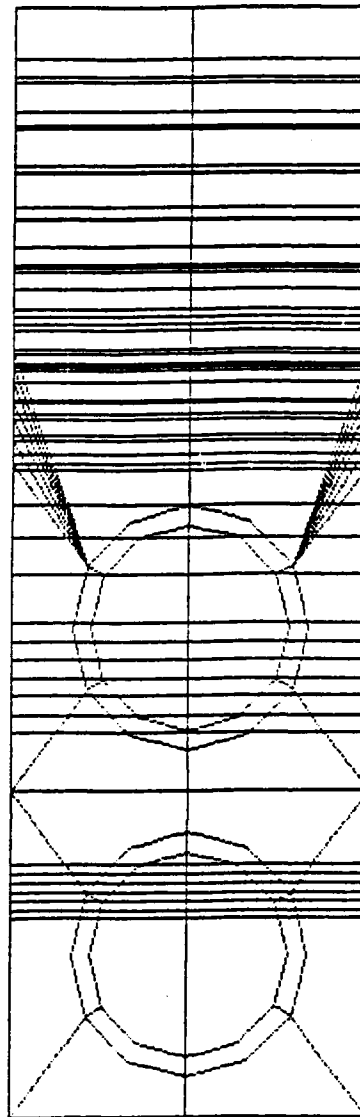


Figure 38. View of 3-dimensional model from the x direction

3D-HEADER  
ORIGINAL —> 0.703

Z  
Y

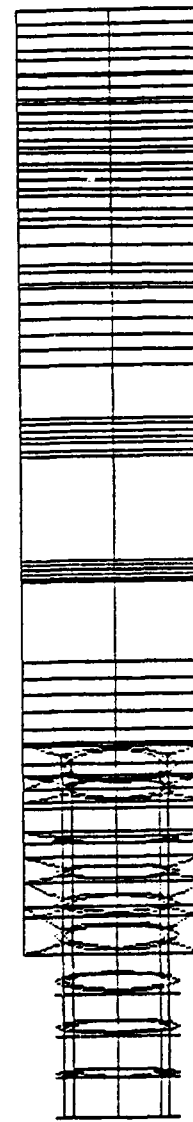


Figure 39. View of 3-dimensional model from the y direction

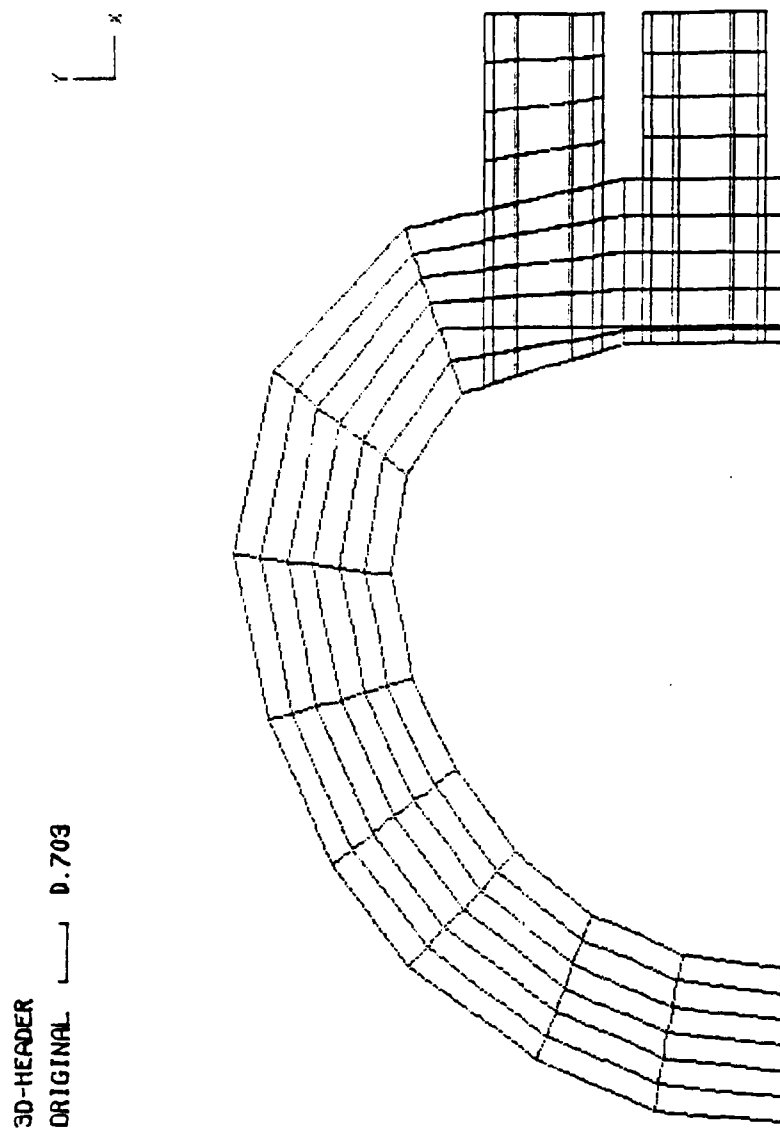


Figure 40. View of 3-dimensional model from the z direction

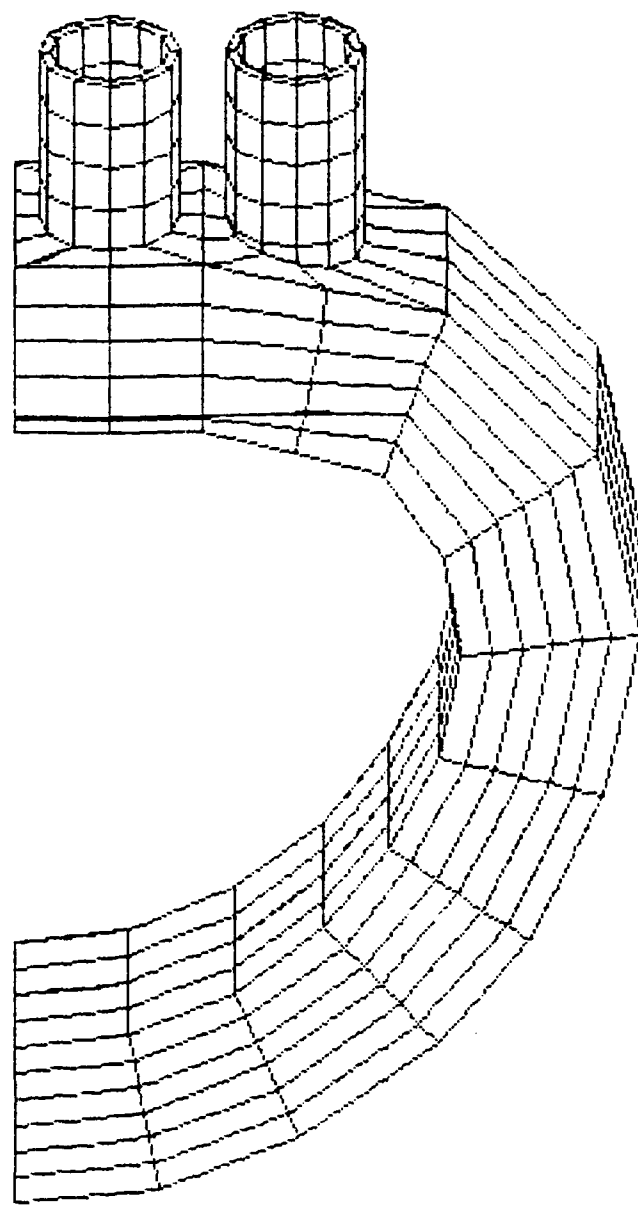


Figure 41. View of model using hidden line removal

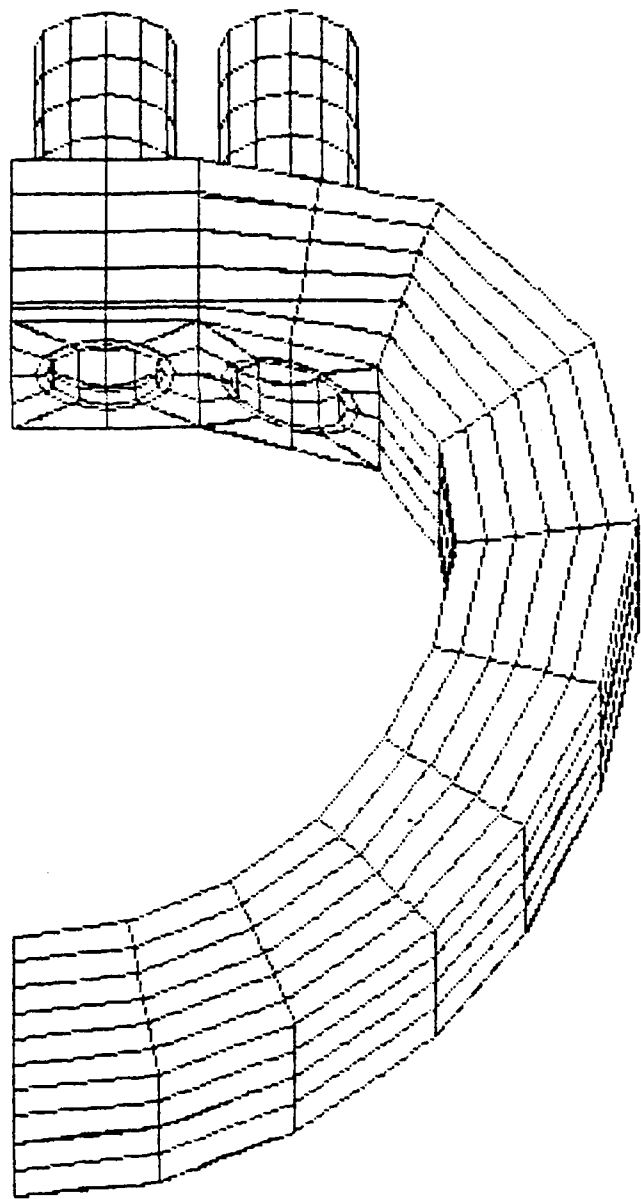


Figure 42. Another view of the model using hidden line removal

It then became necessary to enforce symmetry on either side of the  $z=0$  plane. Every node in this plane was constrained to roll in the plane. It is understood that this enforced symmetry is more costly than modeling only half of the structure. The entire section was modeled to allow a study of unsymmetric temperature loading. The ADINA-IN input file is listed in Appendix I.

Figure 43 on page 60 shows the original and deformed shapes for this loading condition. Table 11 lists the maximum stresses in the area of the weld.

Table 11. MAXIMUM STRESSES  
3-DIMENSIONAL MODEL

Stresses	Internal pressure load
$\sigma_{xx}$ (psi)	.984072E + 03
$\sigma_{yy}$ (psi)	-.111941E + 04
$\sigma_{zz}$ (psi)	.184639E + 04
$\sigma_{xy}$ (psi)	-.487366E + 03
$\sigma_{xz}$ (psi)	.235319E + 03
$\sigma_{yz}$ (psi)	-.814224E + 03

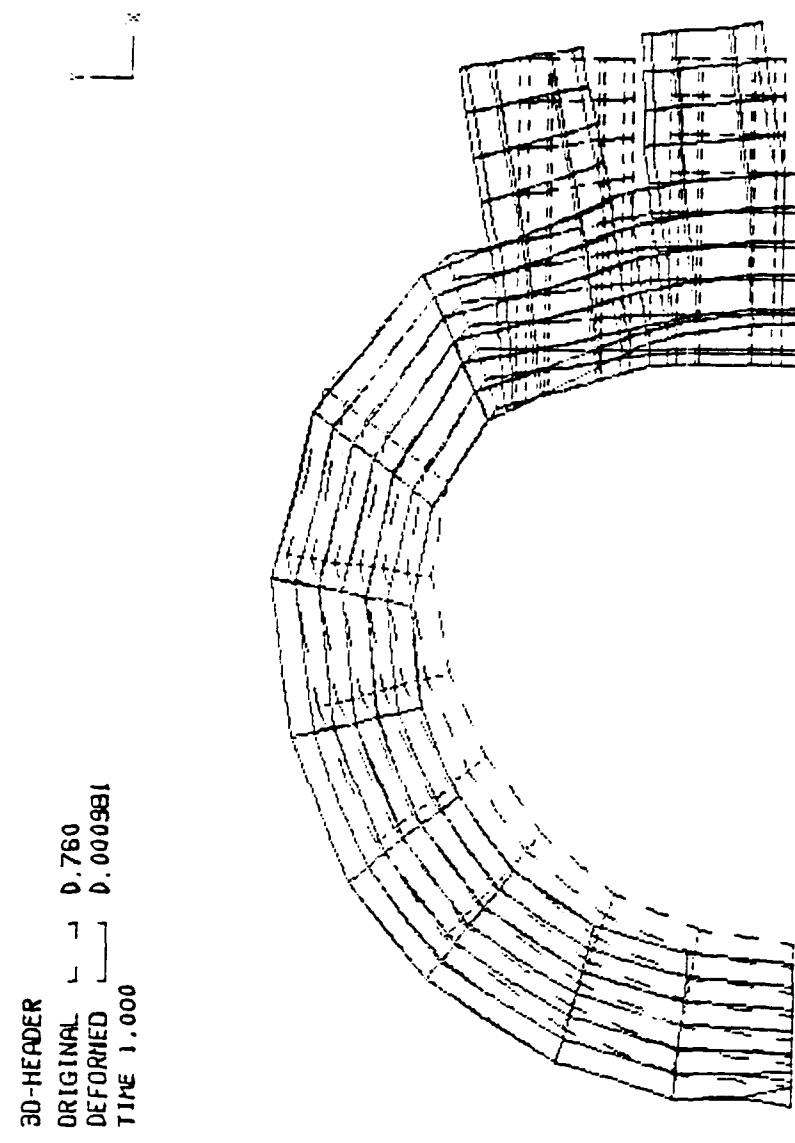


Figure 43. Original and deformed shape of the 3-dimensional model, internal pressure load

## VI. CONCLUSIONS

### A. DISCUSSION OF RESULTS

The maximum stresses obtained for the axisymmetric model were between 137 (ksi) and .46 (ksi), dependent upon the boundary conditions imposed. The axisymmetric model does not adequately represent the physical boundary conditions and the actual stress is somewhere between these two figures.

A 3-dimensional model has been developed which allows an accurate representation of the boundary conditions. The maximum stress for the internal pressure load in the area of the weld was 1.85 (ksi). This model also allows non-symmetric loading to be applied.

### B. OPPORTUNITIES FOR FURTHER RESEARCH

The next step in solving this problem is to obtain results for the thermal loading. The initial loading should be static but the transient loading should also be studied. In studying the transient problem, a consideration should be made of the temperature dependence of the material properties of the structure. Another area for research would be the consideration of creep.

The major attempt of this report was to develop a 3-dimensional model which could be used to investigate the failures that have occurred in the superheater header attachment welds. This model can also be used to investigate any needed design changes. It is hoped that this model will be used for further investigation of this problem.

## APPENDIX A. ADINA-IN PROCEDURES

These procedures are for the VAX/VMS operating system utilizing the plot-10 graphics library.

To operate ADINA-IN in the batch mode, a data file which defines the problem must be created. Assign this data file to a logical unit number and run ADINA-IN.

Now create the database. All of the input to ADINA-IN is stored on this database. The Command is DATAB CREATE. Next read the data file by using the command: READ (logical unit number).

The model can now be plotted using the frame, mesh and plot commands as explained in [Ref. 2: pp. 5.25-1 to 5.25-20]. The CONTROL command must be set to the correct parameters to use graphics. For the VAX-VMS operating system utilizing the plot-10 graphics library, set baudrate = 4800, system = 2, device = 2 and option = 1024. Changes can be made to the model by exiting and changing the data file or by typing in changes interactively. All changes will be saved on the database.

When the problem is properly defined, create the ADINA input file using the command ADINA. Exit ADINA-IN by typing in END.

ADINA-IN will have created two files. FOR001.DAT is the database. This database can best be saved by renaming it to a unique file name. To make changes assign the database to logical unit FOR001 and run ADINA-IN. Use the command DATABASE OPEN and then make any necessary changes.

The second file created by ADINA-IN is FOR002.DAT and this is the input file for ADINA. This file should be renamed to a unique filename and assigned to logical unit number FOR005. Assign an output file to logical unit number FOR006. Ensure there are no FOR\*.\* files in the directory as this can interfere with the operation of ADINA. Now run ADINA. The requested results will be printed in the assigned output file.

## APPENDIX B. ADINA-IN PROCEDURES FOR THE THERMAL STRESS PROBLEM

ADINA-IN is also used for creating the input file for ADINAT. This particular version of ADINA-IN will not create the entire file which necessitates some minor editing of the ADINAT input file before ADINAT can be run.

The temperature loading in this thesis was done by using the LOADS TEMPERATURE command in the ADINA-IN input file. After the problem is defined in ADINA-IN, use the ADINAT command to generate the ADINAT input file.

ADINA-IN again creates two files. FOR001.DAT is the database and FOR002.DAT is the ADINAT input file. Rename these files.

The ADINAT input file must now be edited. Search for the line which has the letters 'KKKKKK'. This line must be deleted and the specific heat entered. The line just above this line must also be deleted and the thermal conductivity entered. Exit the ADINAT input file.

Assign the ADINAT input file to logical unit number FOR005 and assign an output file to logical unit number FOR006. Run ADINAT. ADINAT creates several files, most of which are used for the operation of the code. The final nodal point temperatures and heat fluxes are printed in the output file. The nodal temperatures are also stored in FOR056.DAT. This file must be renamed to a unique filename.

ADINA-IN must now be run again to create the input file for ADINA to solve for the thermal stresses. Assign the nodal temperature file to logical unit number FOR056.

The ADINA-IN input file must be changed. Delete the LOADS TEMPERATURE command and indicate on the MASTER command line that ITP56=1. Run ADINA-IN and read the changed input file. Ensure all FOR\*.\* files are deleted before doing this. Then use the ADINA command to create the ADINA input file. ADINA can now be run as explained in the last paragraph of Appendix A.

## APPENDIX C. ADINA-PLOT PROCEDURES

ADINA created several files besides the assigned output file. Most of these files are used for the operation of the code. File FOR060.DAT is the porthole file for ADINA-PLOT.

Before running ADINA-PLOT, ensure all FOR001.DAT files are deleted and that logical unit number FOR001 is deassigned. Run ADINA-PLOT. First create the database using the DATABASE CREATE command. All of the information in the porthole file is now loaded.

Ensure the control information is correct. The model can now be plotted and the results listed as explained in [Ref. 6].

Exit ADINA-PLOT with the command END. ADINA-PLOT will have created a database with filename FOR001.DAT. Rename this file. To look at the results again, assign the database to logical unit number FOR001 and use the DATABASE OPEN command when running ADINA-PLOT.

## APPENDIX D. VERIFICATION OF ADINA - CANTILEVER BEAM PROBLEM

The cantilever beam problem modeled is shown in Figure 44 on page 66. A moment of 360 k-in is applied to the end of a cantilever beam which is 48 inches long and 12 inches wide.

The classical equations as listed in [Ref. 7: pp. 215 and 737] are:

$$\sigma = My/I \quad (A.1)$$

$$\delta_b = M_o L^2 / 2EI \quad (A.2)$$

The finite element model showing both the original and deformed shapes is shown in Figure 45 on page 67. A nine node plane stress element was used. Table 12 shows a comparison of the results for several nodes. As can be seen, ADINA yields exact results for this problem. The following is the ADINA-IN input file:

Table 12. COMPARISON OF RESULTS

Comparison	Beam Theory	ADINA
displacement of node 10 (inch)	.096	.096
stress at node 1 (psi)	15	15
stress at node 12 (psi)	-15	-15

```
DATAB CREATE
HEAD ' CANTILEVER BEAM'
*
MASTER REACTIONS=YES IDOF=100111
PRINTOUT MAX
ANALYSIS TYPE=STATIC
*
COORDINATES / ENTRIES NODE X Y Z
      1   0   0   0
      5   0   48  0
     15   0   48 12
     11   0   0  12
*
```

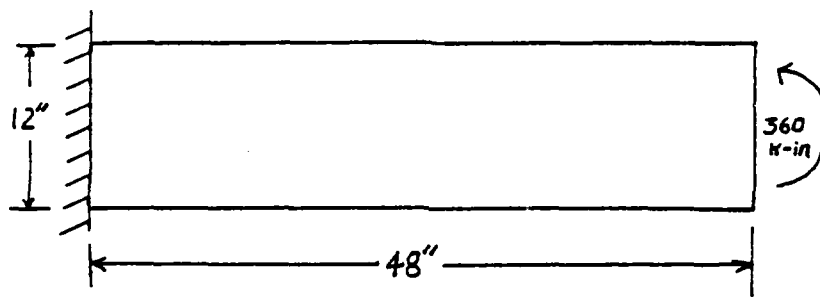


Figure 44. Cantilever beam with concentrated moment

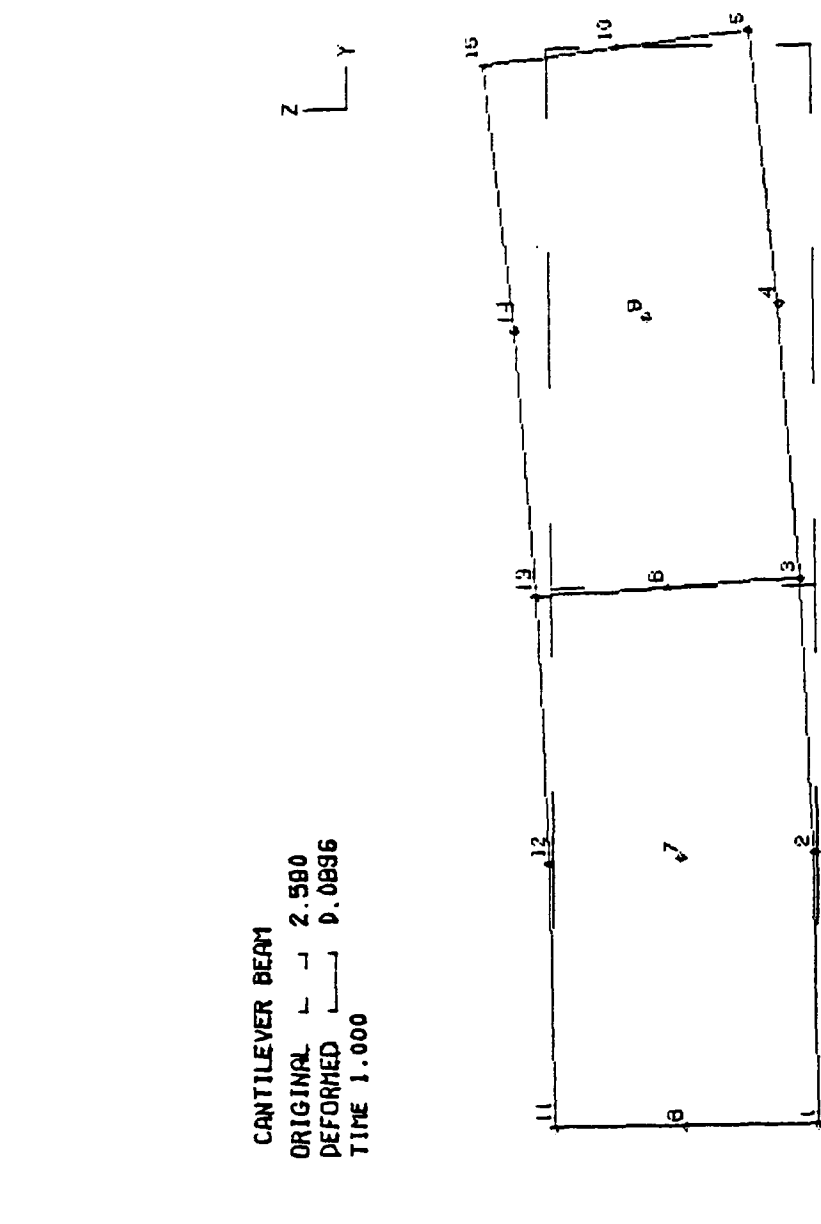


Figure 45. Original and deformed shapes for the cantilever beam

```
MATERIAL 1 ELASTIC E=3E4 NU=0.0 D=1
*
EGROUP 1 PLANE SUBTYPE=STRESS2 RESULTS=STRESSES INT=6
STRESSTABLE N=1 P1=1 P2=2 P3=3 P4=4 P5=5 P6=6 P7=7 P8=8 P9=9
EDATA / ENTRIES EL THICK
    1   1
    2   1
GSURFACE 1 5 15 11 EL1=2 EL2=1 NODES=9
*
BOUNDARIES 111111 TYPE=NODES / 1 6 11
*
LOADS CONCENTRATED
5 2 30
15 2 -30
*
CONTROL B=4800 SYSTEM=2 DEVICE=2 OPTION=1024
CONTROL PLOTE=W PLOTS=N
```

## APPENDIX E. VERIFICATION OF ADINA - ANNULAR DISK PROBLEM

The classical equations for the thermal stresses are listed in [Ref. 8 : p. 259]:

$$\sigma_r = \alpha E [-1/r^2 \int_a^r Tr dr + (r^2 - a^2)/r^2 (b^2 - a^2) \int_a^b Tr dr] \quad (E.1)$$

$$\sigma_\theta = \alpha E [-T + 1/r^2 \int_a^r Tr dr + (r^2 + a^2)/r^2 (b^2 - a^2) \int_a^b Tr dr] \quad (E.2)$$

where:

- a = inner radius, .63 inch
- b = outer radius, 3.0 inch
- T = temperature distribution,  $399.569212 - 86.3436r + 12.16239867r^2$
- E = 29600000 psi
- $\alpha$  = .0000065 in/in/ $^{\circ}$ F

The finite element model showing the original and deformed shapes is shown in Figure 46 on page 70. A nine node plane axisymmetric element was used. Table 13 shows a comparison of the results. The comparison is very good. Most of the difference can be attributed to the fact that the results for the disk theory were computed at the nodes whereas the results for ADINA are calculated at the Gaussian integration points. The following is the ADINA-IN input file:

Table 13. COMPARISON OF RESULTS

r (inch)	Stresses from Disk Theory (psi)	Stresses from ADINA (psi)
.63	$\sigma_\theta = -.139E+05$	$\sigma_\theta = -.120961E+05$
1.815	$\sigma_r = -.2577E+04$	$\sigma_r = -.253146E+04$
1.815	$\sigma_\theta = .1715E+04$	$\sigma_\theta = .169057E+04$
3.0	$\sigma_\theta = .534E+04$	$\sigma_\theta = .511644E+04$

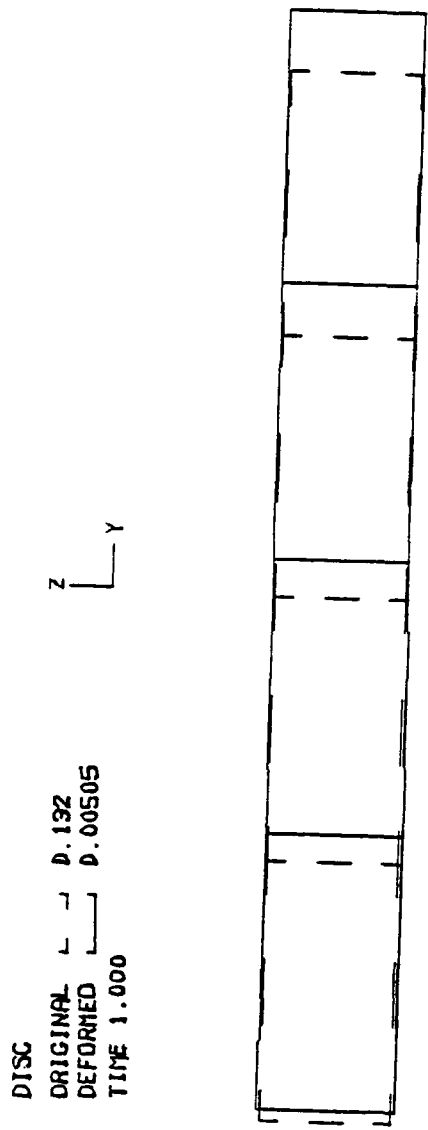


Figure 46. Original and deformed shapes for the disk

```
DATAB CREATE
HEAD 'DISC'
CONTROL B=4800 SYSTEM=2 DEVICE=2 OPTION=1024
CONTROL PLOTE=WAIT PLOTS=NO
*
COORDINATES / ENTRIES NODE X Y Z
    1 0 .63 0
    2 0 .63 .3
    3 0 3.0 0
    4 0 3.0 .3
*
MATERIAL 1 THERMO-ELASTIC
-2000 29600000 .3 .0000065
 2000 29600000 .3 .0000065
*
EGROUP 1 PLANE SU=AXISYMM
GSURFACE 4 2 1 3 EL1=4 EL2=1 NO=9
*
MASTER REACTIONS=YES IDOF=100111
PRINTOUT MAX
ANALYSIS TYPE=STATIC
*
BOUNDARIES 101111 TYPE =NODES/12 STEP 1 TO 20
*
LOADS TEMP TR=0
1 350
2 350
20 350
3 250
4 250
12 250
*
```

## APPENDIX F. VERIFICATION OF ADINA - CHIMNEY PROBLEM

The chimney problem modeled is shown in Figure 47 on page 73. The inside surface is at a uniform temperature of 650 degrees C and the outside surface is at a temperature of 150 degrees C.

The finite element model is shown in Figure 48 on page 74. A nine node plane stress element was used.

A finite difference temperature distribution of this problem was obtained from Professor G. Cantin of the Naval Postgraduate School. The results had converged to the exact solution. Table 14 shows a comparison of the results for several nodes. The comparison is very good. The following is the ADINA-IN input file:

Table 14. RESULTS FOR CHIMNEY PROBLEM

Node	Temperatures from Finite Difference (°C)	Temperatures from ADINA (°C)
10	3.6933026E+02	3.68497E+02
12	3.4661577E+02	3.39891E+02
15	2.5149076E+02	2.52863E+02
16	3.4891941E+02	3.42042E+02
17	3.8732346E+02	4.01579E+02

```
DATAB CREATE
HEAD 'CHIMNEY'
CONTROL B=4800 SYSTEM=2 DEVICE=2 OPTION=1024
CONTROL PLOTE=WAIT PLOTS=NO
```

```
*
```

COORDINATES/ENTRIES	NODE	X	Y	Z
	1	0	2.0	1.5
	2	0	1.0	1.5
	3	0	1.0	1.0
	4	0	2.0	1.0
	5	0	0	1.0
	6	0	0	0
	7	0	2.0	0

```
*
MATERIAL 1 THERMO-ELASTIC
-2000 29600 .3 .0000065
 2000 29600 .3 .0000065
*
```

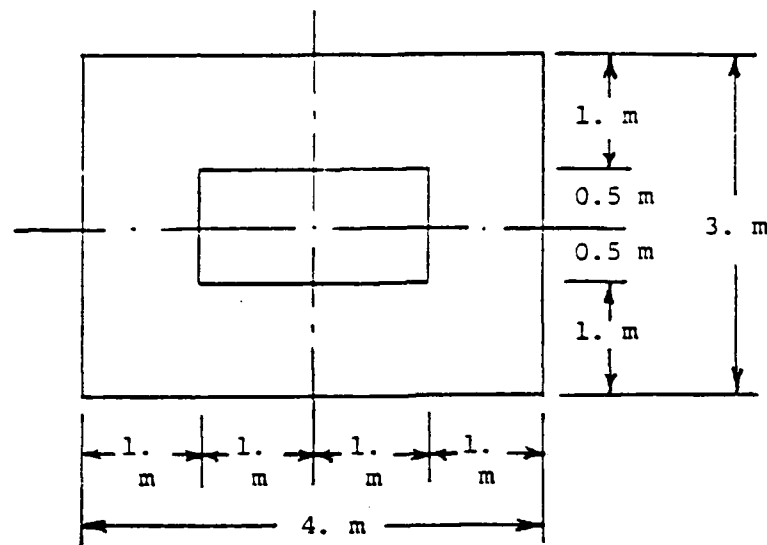


Figure 47. Chimney problem

CHIMNEY  
ORIGINAL — D.129

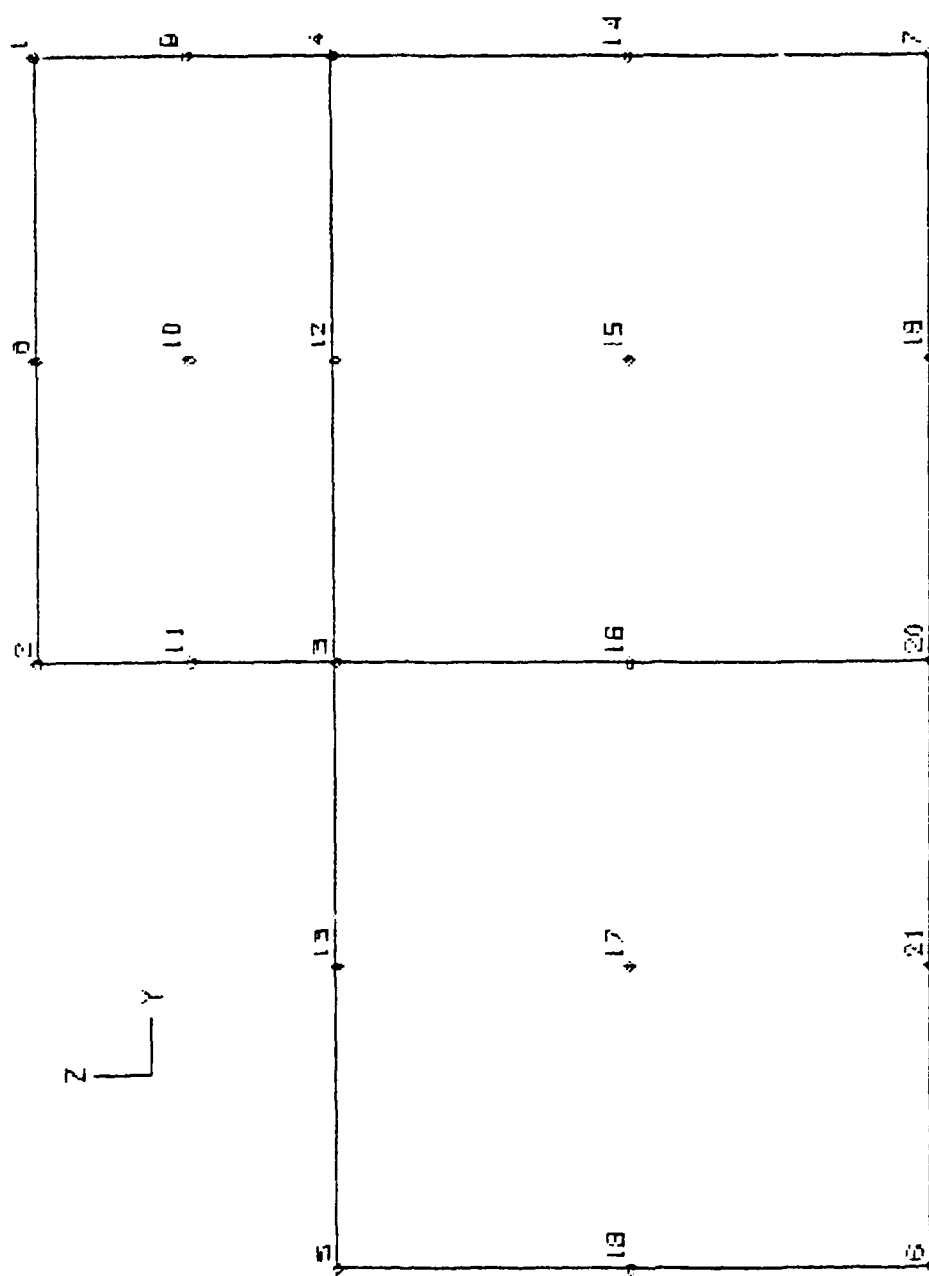


Figure 48. Finite element model of the chimney

EGROUP 1 PLANE SU=STRESS2  
EDATA  
1 1  
2 1  
3 1  
GSURFACE 1 2 3 4 EL1=1 EL2=1 NO=9  
GSURFACE 4 5 6 7 EL1=2 EL2=1 NO=9  
\*  
MASTER REACTIONS=YES IDOF=100111  
PRINTOUT MAX  
ANALYSIS TYPE=STATIC  
\*  
LOADS TEMPERATURE  
1 150  
9 150  
4 150  
14 150  
7 150  
19 150  
20 150  
21 150  
2 650  
11 650  
3 650  
13 650  
5 650  
\*

## APPENDIX G. ADINA-IN INPUT FILE FOR THE AXISYMMETRIC PROBLEM

```

DATAB CREATE
*INPUT FOR THE COARSE MESH, 2-DIMENSIONAL AXISYMMETRIC MODEL
HEAD 'REPEAT HEADER'
CONTROL B=4800 SYSTEM=2 DEVICE=2 OPTION=1024
CONTROL PLOTE=WAIT PLOTS=NO
*COORDINATES ARE DEFINED
COORDINATES / ENTRIES NODE X Y Z
    1   0   .63   3.0
    3   0   .693  3.0
   37   0   .63   2.844
   39   0   .75   2.844
   60   0   .63   2.782
   61   0   .75   2.782
   70   0   .63   1.0
   71   0   .75   1.0
   72   0   .75001 1.0
   85   0   .63   0.0
   87   0   .75   0.0
  100   0   .938  3.0
  200   0   .82   2.837
  152   0   .938  2.97333333
  204   0   .9322366 2.93059481
  211   0   .901  2.88
  210   0   .84513864 2.84814711
  207   0   .792  2.844
  209   0   .813  2.969
  126   0   .938  2.98666666
  178   0   .938  2.96
  208   0   .813  2.844
  206   0   .771  2.844
   50   0   1.0   3.0
     6   0   1.0   2.782
    75   0   1.0   1.0

*MATERIAL PROPERTIES ARE DEFINED
MATERIAL 1 THERMO-ELASTIC
-2000 29600000 .3 .0000065
 2000 29600000 .3 .0000065
*THE ELEMENT IS DEFINED
EGROUP 1 PLANE SU=AXISYMM
*THE MESH FOR THE TUBE IS GENERATED
GSURFACE 3 1 37 39 EL1=1 EL2=3 NO=9 NC=B
GSURFACE 39 37 60 61 EL1=1 EL2=2 NO=9 NC=B
GSURFACE 61 60 70 71 EL1=1 EL2=4 NO=9 NC=B
GSURFACE 71 70 85 87 EL1=1 EL2=1 NO=9 NC=B
*NODES FOR THE WELD ARE GENERATED
LINE A 3 100 NCENTER=200 EL=3 M=1
LINE N 100 204 126 152 178
LINE A 204 211 NCENTER=209 EL=1 M=1
LINE C 100 211 204
LINE A 211 210 NCENTER=209 EL=1 M=1
LINE N 210 39 208 207 206
LINE C 211 39 210
*THE MESH FOR THE WELD IS GENERATED
GSURFACE 100 3 39 211 EL1=3 EL2=3 NO=9 NC=B
*NODES FOR THE HEADER ARE GENERATED
LINE C 100 39 204 211 210
LINE S 50 6 EL=3 M=1
LINE S 6 61 EL=3 M=1
LINE C 50 61 6
*THE MESH FOR THE HEADER IS GENERATED

```

```

GSURFACE 50 100 39 61 EL1=2 EL2=6 NO=9 NC=B
GSURFACE 6 61 72 75 EL1=3 EL2=4 NO=9 NC=N
*PORTIONS OF THE MODEL ARE DEFINED FOR PLOTTING
EZONE TUBE01
1 STEP 1 TO 3
EZONE TUBE02
4 STEP 1 TO 10
EZONE WELD
11 STEP 1 TO 19
EZONE HEAD
20 STEP 1 TO 43
BZONE CLOSE XMIN=0 XMAX=0 YMIN=.63 YMAX=1.0 ZMIN=2.787 ZMAX=3.1
*THE MASTER DEGREES OF FREEDOM ARE DEFINED
MASTER REACTIONS=YES IDOF=100111 DT=1 NSTEP=2 ITP56=1
PRINTOUT MAX
ANALYSIS TYPE=STATIC
*THE LOAD IS APPLIED IN 2 STEPS
TIMEFUNCTION
0 0
2 1
*
TOL T=E I=15 DN=.00001
*NODES ONLY USED FOR GENERATION ARE FIXED, THE BOTTOM RIGHT HAND
*NODE OF THE HEADER IS FIXED
BOUNDARIES 111111 TYPE=NODES /200 209 75
*THE NODES ON THE RIGHT HAND SIDE OF THE HEADER ARE CONSTRAINED TO
*ROLL ONLY IN THE Z DIRECTION
BOUNDARIES 110111 TYPE=NODES / 50 101 STEP 1 TO 105 6
BOUNDARIES 110111 TYPE=NODES / 148 156 163 170 177 185 192
*THE CONTACT SURFACE IS DEFINED
CGROUP 1 CONTACT2 S=AXISYM
CONTACTSURFACE 1
61 155 162 169 176 184 191 198 72
CONTACTSURFACE 2
87 56 71 52 48 45 42 38 34 31 61
CONTACTPAIR 1 T=2 C=1 F=0
*THE INTERNAL PRESSURE LOADING
LOADS ELEMENT
1 -1 700
STEP 1 TO
10 -1 700
1 2 700
13 2 700
12 2 700
11 2 700
21 2 700
20 2 700
*THE LONGITUDINAL TUBE LOAD
LOADS CONCENTRATED
85 3 -25.3
59 3 -101.3
87 3 -25.3
*THE THERMAL LOAD
LOADS TEMP TR=0
50 350.0
101 348.1833333
102 346.3666667
103 344.55
104 342.7333333
105 340.9166667

```

6	339.1
148	327.9625
156	316.825
163	305.6875
170	294.55
177	283.4125
185	272.275
192	261.1375
75	350
1	350
7	350
10	350
13	350
16	350
19	350
37	350
23	350
26	350
29	350
60	350
33	350
36	350
41	350
44	350
47	350
51	350
54	350
70	350
58	350
85	350
2	350
3	350
62	350
63	350
64	350
65	350
66	350
100	350
113	350
112	350
111	350

DATA CREATE  
 \*INPUT FOR THE FINE MESH, 2-DIMENSIONAL AXISYMMETRIC MODEL  
 HEAD 'HEADER'  
 CONTROL B=4800 SYSTEM=2 DEVICE=2 OPTION=1024  
 CONTROL PLOTE=WAIT PLOTS=NO  
 \*COORDINATES ARE DEFINED

COORDINATES / ENTRIES	NODE	X	Y	Z
	1	0	.63	3.0
	3	0	.693	3.0
	37	0	.63	2.844
	39	0	.75	2.844
	60	0	.63	2.782
	61	0	.75	2.782
	70	0	.63	1.0
	71	0	.75	1.0
	72	0	.75001	1.0
	85	0	.63	0.0
	87	0	.75	0.0
	100	0	.938	3.0
	200	0	.82	2.837
	152	0	.938	2.97333333
	256	0	.901	2.88
	248	0	.792	2.844

251	0	.813	2.969
126	0	.938	2.98666666
178	0	.938	2.96
250	0	.813	2.844
246	0	.771	2.844
50	0	1.0	3.0
6	0	1.0	2.782
75	0	1.0	1.0
113	0	.938	2.99333333
139	0	.938	2.98
165	0	.938	2.96666666
249	0	.8025	2.844
247	0	.7815	2.844
245	0	.7605	2.844

\*MATERIAL PROPERTIES ARE DEFINED  
 MATERIAL 1 ELASTIC E=296000000 NU=.3  
 \*THE ELEMENT IS DEFINED  
 EGROUP 1 PLANE SU=AXISYMM  
 \*THE MESH FOR THE TUBE IS GENERATED  
 GSURFACE 3 1 37 39 EL1=2 EL2=6 NO=9  
 GSURFACE 39 37 60 61 EL1=2 EL2=4 NO=9  
 GSURFACE 61 60 70 71 EL1=2 EL2=8 NO=9  
 GSURFACE 71 70 85 87 EL1=2 EL2=2 NO=9  
 \*NODES FOR THE WELD ARE GENERATED  
 LINE A 3 100 NCENTER=200 EL=6 M=1  
 LINE N 100 178 113 126 139 152 165  
 LINE A 178 256 NCENTER=251 EL=3 M=1  
 LINE C 100 256 178  
 LINE A 256 250 NCENTER=251 EL=3 M=1  
 LINE N 250 39 249 248 247 246 245  
 LINE C 256 39 250  
 \*THE MESH FOR THE WELD IS GENERATED  
 GSURFACE 100 3 39 256 EL1=6 EL2=6 NO=9  
 \*NODES FOR THE HEADER ARE GENERATED  
 LINE C 100 39 178 256 250  
 LINE S 50 6 EL=6 M=1  
 LINE S 6 61 EL=6 M=1  
 LINE C 50 61 6  
 \*THE MESH FOR THE HEADER IS GENERATED  
 GSURFACE 50 100 39 61 EL1=4 EL2=12 NO=9  
 GSURFACE 6 61 72 75 EL1=6 EL2=8 NO=9 NC=N  
 \*PORTIONS OF THE TUBE ARE DEFINED FOR PLOTTING  
 EZONE TUBE01  
 1 STEP 1 TO 12  
 EZONE TUBE02  
 13 STEP 1 TO 44  
 EZONE WELD  
 45 STEP 1 TO 80  
 EZONE HEAD  
 81 STEP 1 TO 256  
 BZONE CLOSE XMIN=0 XMAX=0 YMIN=.63 YMAX=1.094 ZMIN=2.688 ZMAX=3.1  
 BZONE HEAD01 XMIN=0 XMAX=0 YMIN=1.094 YMAX=2.0 ZMIN=2.688 ZMAX=3.0  
 BZONE HEAD02 XMIN=0 XMAX=0 YMIN=1.094 YMAX=2.0 ZMIN=1.0 ZMAX=2.688  
 BZONE HEAD03 XMIN=0 XMAX=0 YMIN=.63 YMAX=1.094 ZMIN=1.0 ZMAX=2.688  
 BZONE TUBE XMIN=0 XMAX=0 YMIN=.63 YMAX=.693 ZMIN=0 ZMAX=1.0  
 \*THE MASTER DEGREES OF FREEDOM ARE DEFINED  
 MASTER REACTIONS=YES IDOF=100111 DT=1 NSTEP=2  
 PRINTOUT MAX  
 ANALYSIS TYPE=STATIC  
 \*THE LOAD IS APPLIED IN 2 STEPS  
 TIMEFUNCTION  
 0 0  
 2 1  
 \*  
 TOL T=E I=15 DN=.00001  
 \*NODES USED FOR GENERATION ARE FIXED, THE BOTTOM RIGHT HAND NODE  
 \*OF THE HEADER IS FIXED  
 BOUNDARIES 111111 TYPE=NODES / 200 251 75

\*THE NODES AT THE RIGHT HAND SIDE OF THE HEADER ARE CONSTRAINED TO  
 \*ROLL ONLY IN THE Z-DIRECTION  
 BOUNDARIES 110111 TYPE-NODES/ 50 368 STEP 1 TO 378 6 558 STEP 13 TO 740  
 \*THE CONTACT SURFACES ARE DEFINED  
 CGROUP 1 CONTACT2 S=AXISYM  
 CONTACTSURFACE 1  
 87 210 205 199 71 191 186 181 175 170 164 159 154 148 143 137 132 127 121 116 61  
 CONTACTSURFACE 2  
 61 570 583 596 609 622 635 648 661 674 687 700 713 726 739 752 72  
 CONTACTPAIR 1 T=2 C=1 F=0  
 \*THE INTERNAL PRESSURE LOAD  
 LOADS ELEMENT  
 2 -1 700  
 STEP 2 TO  
 40 -1 700  
 2 2 700  
 1 2 700  
 41 2 700  
 STEP 1 TO  
 46 2 700  
 77 2 700  
 STEP 1 TO  
 80 2 700  
 \*THE LONGITUDINAL TUBE LOAD  
 LOADS CONCENTRATED  
 85 3 -12.66666666  
 217 3 -50.66666666  
 216 3 -25.33333333  
 215 3 -50.66666666  
 87 3 -12.66666666  
 \*THE THERMAL LOAD  
 LOADS TEMP TR=0  
 50 350  
 368 349.0916667  
 369 348.1833333  
 370 347.275  
 371 346.3666667  
 372 345.4583333  
 373 344.55  
 374 343.5416667  
 375 342.7333333  
 376 341.825  
 377 340.9166667  
 378 340.0083333  
 6 339.1  
 558 333.53125  
 571 327.9625  
 584 322.39375  
 597 316.825  
 610 311.25625  
 623 305.6875  
 636 300.11875  
 649 294.55  
 662 288.98125  
 675 283.4125  
 688 277.84375  
 701 272.275  
 714 266.70625  
 727 261.1375  
 740 255.56875  
 75 250  
 1 350  
 STEP 1 TO  
 5 350  
 218 350  
 STEP 1 TO  
 228 350

100 350  
390 350  
STEP 1 TO  
396 350  
50 350  
11 350  
STEP 5 TO  
36 350  
43 350  
48 350  
54 350  
59 350  
66 350  
37 350  
78 350  
83 350  
90 350  
95 350  
101 350  
106 350  
111 350  
60 350  
120 350  
125 350  
131 350  
136 350  
142 350  
147 350  
153 350  
158 350  
163 350  
169 350  
174 350  
180 350  
185 350  
190 350  
195 350  
70 350  
204 350  
209 350  
214 350  
85 350  
\*

## APPENDIX H. ADINA-IN INPUT FILE FOR THE 3-DIMENSIONAL CONTACT SURFACE

\*THESE ARE THE CONTACT SURFACES FOR THE 3-DIMENSIONAL MODEL  
CGROUP 1 CONTACT3

\*CONTACTSURFACE 1 IS THE HEADER AROUND THE INNER TUBE  
CONTACTSURFACE 1

1	123	124	970	969
2	969	970	982	981
3	981	982	994	993
4	993	994	69	68
5	124	125	971	970
6	970	971	983	982
7	982	983	995	994
8	994	995	70	69
9	125	126	1021	971
10	971	1021	1029	983
11	983	1029	1037	995
12	995	1037	71	70
13	126	127	1022	1021
14	1021	1022	1030	1029
15	1029	1030	1038	1037
16	1037	1038	72	71
17	127	128	1057	1022
18	1022	1057	1065	1030
19	1030	1065	1073	1038
20	1038	1073	73	72
21	128	129	1058	1057
22	1057	1058	1066	1065
23	1065	1066	1074	1073
24	1073	1074	74	73
25	129	130	1093	1058
26	1058	1093	1101	1066
27	1066	1101	1109	1074
28	1074	1109	75	74
29	130	131	1094	1093
30	1093	1094	1102	1101
31	1101	1102	1110	1109
32	1109	1110	76	75
33	131	132	1129	1094
34	1094	1129	1137	1102
35	1102	1137	1145	1110
36	1110	1145	77	76
37	132	11	1130	1129
38	1129	1130	1138	1137
39	1137	1138	1146	1145
40	1145	1146	6	77

41 11 122 1161 1130  
42 1130 1161 1165 1138  
43 1138 1165 1169 1146  
44 1146 1169 67 6  
45 122 123 969 1161  
46 1161 969 981 1165  
47 1165 981 993 1169  
48 1169 993 68 67

\*CONTACTSURFACE 2 IS THE HEADER AROUND THE OUTER TUBE  
CONTACTSURFACE 2

1 585 586 1354 1323  
2 1323 1354 1358 1331  
3 1331 1358 1362 1339  
4 1339 1362 531 530  
5 586 587 1180 1354  
6 1354 1180 1188 1358  
7 1358 1188 1196 1362  
8 1362 1196 532 531  
9 587 588 1181 1180  
10 1180 1181 1189 1188  
11 1188 1189 1197 1196  
12 1196 1197 533 532  
13 588 589 1182 1181  
14 1181 1182 1190 1189  
15 1189 1190 1198 1197  
16 1197 1198 534 533  
17 589 590 1212 1182  
18 1182 1212 1218 1190  
19 1190 1218 1224 1198  
20 1198 1224 535 534  
21 590 591 1213 1212  
22 1212 1213 1219 1218  
23 1218 1219 1225 1224  
24 1224 1225 536 535  
25 591 592 1250 1213  
26 1213 1250 1258 1219  
27 1219 1258 1266 1225  
28 1225 1266 537 536  
29 592 593 1251 1250  
30 1250 1251 1259 1258  
31 1258 1259 1267 1266  
32 1266 1267 538 537  
33 593 594 1286 1251  
34 1251 1286 1294 1259  
35 1259 1294 1302 1267  
36 1267 1302 539 538  
37 594 473 1287 1286  
38 1286 1287 1295 1294  
39 1294 1295 1303 1302  
40 1302 1303 468 539  
41 473 584 1322 1287

42 1287 1322 1330 1295  
43 1295 1330 1338 1303  
44 1303 1338 529 468  
45 584 585 1323 1322  
46 1322 1323 1331 1330  
47 1330 1331 1339 1338  
48 1338 1339 530 529  
\*CONTACTSURFACE 3 IS THE INNER TUBE  
CONTACTSURFACE 3  
1 195 237 238 196  
2 237 90 91 238  
3 90 297 298 91  
4 297 339 340 298  
5 339 381 382 340  
6 381 68 69 382  
7 196 238 239 197  
8 238 91 92 239  
9 91 298 299 92  
10 298 340 341 299  
11 340 382 383 341  
12 382 69 70 383  
13 197 239 240 198  
14 239 92 93 240  
15 92 299 300 93  
16 299 341 342 300  
17 341 383 384 342  
18 383 70 71 384  
19 198 240 241 199  
20 240 93 94 241  
21 93 300 301 94  
22 300 342 343 301  
23 342 384 385 343  
24 384 71 72 385  
25 199 241 242 200  
26 241 94 95 242  
27 94 301 302 95  
28 301 343 344 302  
29 343 385 386 344  
30 385 72 73 386  
31 200 242 243 201  
32 242 95 96 243  
33 95 302 303 96  
34 302 344 345 303  
35 344 386 387 345  
36 386 73 74 387  
37 201 243 244 202  
38 243 96 97 244  
39 96 303 304 97  
40 303 345 346 304  
41 345 387 388 346  
42 387 74 75 388  
43 202 244 245 203

44 244 97 98 245  
45 97 304 305 98  
46 304 346 347 305  
47 346 388 389 347  
48 388 75 76 389  
49 203 245 246 204  
50 245 98 99 246  
51 98 305 306 99  
52 305 347 348 306  
53 347 389 390 348  
54 389 76 77 390  
55 204 246 235 193  
56 246 99 8 235  
57 99 306 295 8  
58 306 348 337 295  
59 348 390 379 337  
60 390 77 6 379  
61 193 235 236 194  
62 235 8 89 236  
63 8 295 296 89  
64 295 337 338 296  
65 337 379 380 338  
66 379 6 67 380  
67 194 236 237 195  
68 236 89 90 237  
69 89 296 297 90  
70 296 338 339 297  
71 338 380 381 339  
72 380 67 68 381

\*CONTACTSURFACE 4 IS THE OUTER TUBE

CONTACTSURFACE 4  
1 657 699 700 658  
2 699 552 553 700  
3 552 759 760 553  
4 759 801 802 760  
5 801 843 844 802  
6 843 530 531 844  
7 658 700 701 659  
8 700 553 554 701  
9 553 760 761 554  
10 760 802 803 761  
11 802 844 845 803  
12 844 531 532 845  
13 659 701 702 660  
14 701 554 555 702  
15 554 761 762 555  
16 761 803 804 762  
17 803 845 846 804  
18 845 532 533 846  
19 660 702 703 661  
20 702 555 556 703  
21 555 762 763 556

22	762	804	805	763
23	804	846	847	805
24	846	533	534	847
25	661	703	704	662
26	703	556	557	704
27	556	763	764	557
28	763	805	806	764
29	805	847	848	806
30	847	534	535	848
31	662	704	705	663
32	704	557	558	705
33	557	764	765	558
34	764	806	807	765
35	806	848	849	807
36	848	535	536	849
37	663	705	706	664
38	705	558	559	706
39	558	765	766	559
40	765	807	808	766
41	807	849	850	808
42	849	536	537	850
43	664	706	707	665
44	706	559	560	707
45	559	766	767	560
46	766	808	809	767
47	808	850	851	809
48	850	537	538	851
49	665	707	708	566
50	707	560	561	708
51	560	767	768	561
52	767	809	810	768
53	809	851	852	810
54	851	538	539	852
55	666	708	697	655
56	708	561	470	697
57	561	768	757	470
58	768	810	799	757
59	810	852	841	799
60	852	539	468	841
61	655	697	698	656
62	697	470	551	698
63	470	757	758	551
64	757	799	800	758
65	799	841	842	800
66	841	468	529	842
67	656	698	699	657
68	698	551	552	699
69	551	758	759	552
70	758	800	801	759
71	800	842	843	801
72	842	529	530	843

## APPENDIX I. ADINA-IN INPUT FILE FOR THE 3-DIMENSIONAL PROBLEM

```

DATAB CREATE
HEAD '3D-HEADER'
CONTROL B=4800 SYSTEM=2 DEVICE=2 OPTION=1024
CONTROL PLOTE=WAIT PLOTS=NO
*THE COORDINATES FOR THE INNER TUBE ARE DEFINED
SYSTEM 1 TYPE=CYLINDRICAL X=9.4 Y=1 Z=1.125
COORDINATES /ENTRIES NODE R THETA XL
    1   .63   0   0
    2   .75   0   0
    3   .63   0   .156
    4   .75   0   .156
    5   .63   0   .218
    6   .75   0   .218
    7   .63   0   2.0
    8   .75   0   2.0
    9   .63   0   4.0
    10  .75   0   4.0
    11  .75001 0   2.0
LINE CYLINDRICAL 1 1 6 1
LINE CYLINDRICAL 2 2 6 1
LINE CYLINDRICAL 3 3 6 1
LINE CYLINDRICAL 4 4 6 1
LINE CYLINDRICAL 5 5 6 1
LINE CYLINDRICAL 6 6 6 1
LINE CYLINDRICAL 7 7 6 1
LINE CYLINDRICAL 8 8 6 1
LINE CYLINDRICAL 9 9 6 1
LINE CYLINDRICAL 10 10 6 1
LINE CYLINDRICAL 11 11 6 1
*THE MASTER DEGREES OF FREEDOM ARE DEFINED
MASTER REACTIONS=YES IDOF=000111
PRINTOUT V=MIN IO=0
ANALYSIS TYPE=STATIC
VIEW 1 X=1
VIEW 2 X=-1
VIEW 3 Y=1
VIEW 4 Y=-1
VIEW 5 Z=1
VIEW 6 Z=-1
*THE MATERIAL PROPERTIES ARE DEFINED
MATERIAL 1 ELASTIC E=29600000 NU=.3
*THE ELEMENT IS DEFINED
EGROUP 1 SOLID
STRESSTABLE 1 1 2 3 4 5 6 7 8 21
EDATA/ENTRIES EL TABLE PRINT
    1   1   YES
    STEP 1 TO
    288  1   YES
*THE MESH FOR THE INNER TUBE IS GENERATED
GVOLUME 10 10 9 9 8 8 7 7 EL1=6 EL2=1 EL3=4 NO=20
GVOLUME 8 8 7 7 6 6 5 5 EL1=6 EL2=1 EL3=4 NO=20
GVOLUME 6 6 5 5 4 4 3 3 EL1=6 EL2=1 EL3=1 NO=20
GVOLUME 4 4 3 3 2 2 1 1 EL1=6 EL2=1 EL3=1 NO=20
*THE COORDINATES FOR THE OUTER TUBE ARE DEFINED
SYSTEM 2 TYPE=CYLINDRICAL X=9.4 Y=3.0 Z=1.125

```

16-1238 448

2-DIMENSIONAL AXISYMMETRIC AND 3-DIMENSIONAL FINITE  
ELEMENT STRESS ANALYSIS OF THE LHA-1 CLASS SUPERHEATER

HEADER(U) NAVAL POSTGRADUATE SCHOOL MONTEREY CA

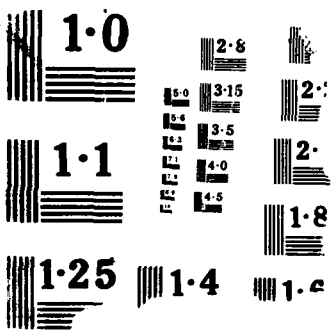
UNCLASSIFIED

D R KITCHIN MAR 88

F/G 20/11

NL

111  
1111  
11111  
111111



COORDINATES / ENTRIES	NODE	R	THETA	XL
	463	.63	0	-.4564
	464	.75	0	-.49
	465	.63	0	-.09327705
	466	.75	0	-.11162873
	479	.63	180	-.1036
	490	.75	180	-.07
	467	.63	0	.218
	468	.75	0	.218
	469	.63	0	1.64381482
	470	.75	0	1.61759259
	471	.63	0	4.0
	472	.75	0	4.0
	473	.75001	0	1.61759041
	589	.75001	180	1.94537256
	474	.63	30	-.43276688
	475	.63	60	-.3682
	476	.63	90	-.28
	477	.63	120	-.1918
	478	.63	150	-.12723312
	480	.63	210	-.12723312
	481	.63	240	-.1918
	482	.63	270	-.28
	483	.63	300	-.3682
	484	.63	330	-.43276688
	485	.75	30	-.46186535
	486	.75	60	-.385
	487	.75	90	-.28
	488	.75	120	-.175
	489	.75	150	-.09813465
	491	.75	210	-.09813465
	492	.75	240	-.175
	493	.75	270	-.28
	494	.75	300	-.385
	495	.75	330	-.46186535
	584	.75001	30	1.63954765
	585	.75001	60	1.69953594
	586	.75001	90	1.78148148
	587	.75001	120	1.86342702
	588	.75001	150	1.92341531
	590	.75001	210	1.92341531
	591	.75001	240	1.86342702
	592	.75001	270	1.78148148
	593	.75001	300	1.69953594
	594	.75001	330	1.63954765
	496	.63	30	-.08036908
	497	.63	60	-.04510387
	498	.63	90	.0030693
	499	.63	120	.05124247
	500	.63	150	.08650768
	501	.63	180	.09941564
	502	.63	210	.08650768
	503	.63	240	.05124247
	504	.63	270	.0030693
	505	.63	300	-.04510387
	506	.63	330	-.08036908
	507	.75	30	-.09626212
	508	.75	60	-.05427972
	509	.75	90	.0030693
	510	.75	120	.06041831
	511	.75	150	.10240071
	512	.75	180	.11776732
	513	.75	210	.10240071
	514	.75	240	.06041831
	515	.75	270	.0030693

516	.75	300	-.05427972
517	.75	330	-.09626212
540	.63	30	1.66225867
541	.63	60	1.71264813
542	.63	90	1.78148148
543	.63	120	1.85031484
544	.63	150	1.9007043
545	.63	180	1.91914817
546	.63	210	1.9007043
547	.63	240	1.85031484
548	.63	270	1.78148148
549	.63	300	1.71264813
550	.63	330	1.66225867
551	.75	30	1.63954951
552	.75	60	1.69953704
553	.75	90	1.78148148
554	.75	120	1.86342593
555	.75	150	1.92341346
556	.75	180	1.94537037
557	.75	210	1.92341346
558	.75	240	1.86342593
559	.75	270	1.78148148
560	.75	300	1.69953704
561	.75	330	1.63954951

\*

```

LINE NODES 463 463 474 475
        476 STEP 1 TO 484
LINE NODES 464 464 485 486
        487 STEP 1 TO 495
LINE NODES 465 465 496 497
        498 STEP 1 TO 506
LINE NODES 466 466 507 508
        509 STEP 1 TO 517
LINE CYLINDRICAL 467 467 6 1
LINE CYLINDRICAL 468 468 6 1
LINE NODES 469 469 540 541
        542 STEP 1 TO 550
LINE NODES 470 470 551 552
        553 STEP 1 TO 561
LINE CYLINDRICAL 471 471 6 1
LINE CYLINDRICAL 472 472 6 1
LINE NODES 473 473 584 585
        586 STEP 1 TO 594

```

\*THE MESH FOR THE OUTER TUBE IS GENERATED

```

GVOLUME 472 472 471 471 470 470 469 469 ELL=6 EL1=6 EL2=1 EL3=4 NO=20
GVOLUME 470 470 469 469 468 468 467 467 ELL=6 EL1=6 EL2=1 EL3=4 NO=20
GVOLUME 468 468 467 467 466 466 465 465 ELL=6 EL1=6 EL2=1 EL3=1 NO=20
GVOLUME 466 466 465 465 464 464 463 463 ELL=6 EL1=6 EL2=1 EL3=1 NO=20

```

\*THE COORDINATES FOR THE HEADER AROUND THE TUBES ARE DEFINED

SYSTEM N=3 TYPE=CARTESIAN X=9.4 Y=0 Z=0

COORDINATES / ENTRIES NODE X Y Z

\*INNER TUBE HEADER NODES

925	0.0	0.0	0.0
926	.156	0.0	0.0
927	.218	0.0	0.0
928	2.0	0.0	0.0
929	0.0	0.0	1.125
930	.156	0.0	1.125
931	.218	0.0	1.125
932	2.0	0.0	1.125

933	0.0	0.0	2.25
934	.156	0.0	2.25
935	.218	0.0	2.25
936	2.0	0.0	2.25
937	0.0	2.0	0.0
938	.156	2.0	0.0
939	.218	2.0	0.0
940	2.0	2.0	0.0
941	0.0	2.0	1.125
942	.156	2.0	1.125
943	.218	2.0	1.125
944	2.0	2.0	1.125
945	0.0	2.0	2.25
946	.156	2.0	2.25
947	.218	2.0	2.25
948	2.0	2.0	2.25

\*NODES OF THE CENTERS OF THE TUBES FOR MESH GENERATION

949	0.0	1.0	1.125
950	.156	1.0	1.125
951	.218	1.0	1.125
952	2.0	1.0	1.125
953	0.0	3.0	1.125
954	.156	3.0	1.125
955	.218	3.0	1.125
956	2.0	3.0	1.125

\*OUTER TUBE HEADER NODES

1230	1.41	4.7	2.25
1231	.218	4.2764467	2.25
1232	-.171	4.13822335	2.25
1233	-.56	4.0	2.25
1234	1.41	4.7	1.125
1235	.218	4.2764467	1.125
1236	-.171	4.13822335	1.125
1237	-.56	4.0	1.125
1238	1.41	4.7	0.0
1239	.218	4.2764467	0.0
1240	-.171	4.13822335	0.0
1241	-.56	4.0	0.0

\*GENERATION OF THE MESH FOR THE INNER TUBE HEADER

LINE NODES 123 125 124

LINE ARC 68 70 NCEN=951 EL=1 M=1 NCO=ALL

LINE ARC 46 48 NCEN=950 EL=1 M=1 NCO=ALL

LINE ARC 24 26 NCEN=949 EL=1 M=1 NCO=ALL

GVOLUME 948 936 125 123 947 935 70 68 EL1=1 EL2=1 EL3=4 NC=N

GVOLUME 947 935 70 68 946 934 48 46 EL1=1 EL2=1 EL3=1 NC=A

GVOLUME 946 934 48 46 945 933 26 24 EL1=1 EL2=1 EL3=1 NC=A

\*

LINE NODES 125 127 126

LINE ARC 70 72 NCEN=951 EL=1 M=1 NCO=ALL

LINE ARC 48 50 NCEN=950 EL=1 M=1 NCO=ALL

LINE ARC 26 28 NCEN=949 EL=1 M=1 NCO=ALL

GVOLUME 936 932 127 125 935 931 72 70 EL1=1 EL2=1 EL3=4 NC=N

GVOLUME 935 931 72 70 934 930 50 48 EL1=1 EL2=1 EL3=1 NC=A

GVOLUME 934 930 50 48 933 929 28 26 EL1=1 EL2=1 EL3=1 NC=A

\*

LINE NODES 127 129 128

LINE ARC 72 74 NCEN=951 EL=1 M=1 NCO=ALL

LINE ARC 50 52 NCEN=950 EL=1 M=1 NCO=ALL

LINE ARC 28 30 NCEN=949 EL=1 M=1 NCO=ALL

GVOLUME 932 928 129 127 931 927 74 72 EL1=1 EL2=1 EL3=4 NC=N

```

GVOLUME 931 927 74 72 930 926 52 50 EL1=1 EL2=1 EL3=1 NC=A
GVOLUME 930 926 52 50 929 925 30 28 EL1=1 EL2=1 EL3=1 NC=A
*
LINE NODES 129 131 130
LINE ARC 74 76 NCEN=951 EL=1 M=1 NCO=ALL
LINE ARC 52 54 NCEN=950 EL=1 M=1 NCO=ALL
LINE ARC 30 32 NCEN=949 EL=1 M=1 NCO=ALL
GVOLUME 928 940 131 129 927 939 76 74 EL1=1 EL2=1 EL3=4 NC=N
GVOLUME 927 939 76 74 926 938 54 52 EL1=1 EL2=1 EL3=1 NC=A
GVOLUME 926 938 54 52 925 937 32 30 EL1=1 EL2=1 EL3=1 NC=A
*
LINE NODES 131 11 132
LINE ARC 76 6 NCEN=951 EL=1 M=1 NCO=ALL
LINE ARC 54 4 NCEN=950 EL=1 M=1 NCO=ALL
LINE ARC 32 2 NCEN=949 EL=1 M=1 NCO=ALL
GVOLUME 940 944 11 131 939 943 6 76 EL1=1 EL2=1 EL3=4 NC=N
GVOLUME 939 943 6 76 938 942 4 54 EL1=1 EL2=1 EL3=1 NC=A
GVOLUME 938 942 4 54 937 941 2 32 EL1=1 EL2=1 EL3=1 NC=A
*
LINE NODES 11 123 122
LINE ARC 6 68 NCEN=951 EL=1 M=1 NCO=ALL
LINE ARC 4 46 NCEN=950 EL=1 M=1 NCO=ALL
LINE ARC 2 24 NCEN=949 EL=1 M=1 NCO=ALL
GVOLUME 944 948 123 11 943 947 68 6 EL1=1 EL2=1 EL3=4 NC=N
GVOLUME 943 947 68 6 942 946 46 4 EL1=1 EL2=1 EL3=1 NC=A
GVOLUME 942 946 46 4 941 945 24 2 EL1=1 EL2=1 EL3=1 NC=A
*GENERATION OF THE MESH FOR THE OUTER TUBE HEADER
LINE NODES 587 589 588
LINE NODES 532 534 533
LINE NODES 510 512 511
LINE NODES 488 490 489
GVOLUME 948 944 589 587 947 943 534 532 EL1=1 EL2=1 EL3=4 NC=N
LINE NODES 532 510 891
GVOLUME 947 943 534 532 946 942 512 510 EL1=1 EL2=1 EL3=1 NC=A
LINE NODES 510 488 909
GVOLUME 946 942 512 510 945 941 490 488 EL1=1 EL2=1 EL3=1 NC=A
*
LINE NODES 589 591 590
LINE NODES 534 536 535
LINE NODES 512 514 513
LINE NODES 490 492 491
GVOLUME 944 940 591 589 943 939 536 534 EL1=1 EL2=1 EL3=4 NC=N
LINE NODES 536 514 893
GVOLUME 943 939 536 534 942 938 514 512 EL1=1 EL2=1 EL3=1 NC=A
LINE NODES 514 492 911
GVOLUME 942 938 514 512 941 937 492 490 EL1=1 EL2=1 EL3=1 NC=A
*
LINE NODES 591 593 592
LINE NODES 536 538 537
LINE NODES 514 516 515
LINE NODES 492 494 493
GVOLUME 940 1238 593 591 939 1239 538 536 EL1=1 EL2=1 EL3=4 NC=N
LINE NODES 538 516 894
GVOLUME 939 1239 538 536 938 1240 516 514 EL1=1 EL2=1 EL3=1 NC=A
LINE NODES 516 494 912
GVOLUME 938 1240 516 514 937 1241 494 492 EL1=1 EL2=1 EL3=1 NC=A
*
LINE NODES 593 473 594
LINE NODES 538 468 539
LINE NODES 516 466 517

```

LINE NODES 494 464 495  
GVOLUME 1238 1234 473 593 1239 1235 468 538 EL1=1 EL2=1 EL3=4 NC=N  
GVOLUME 1239 1235 468 538 1240 1236 466 516 EL1=1 EL2=1 EL3=1 NC=A  
GVOLUME 1240 1236 466 516 1241 1237 464 494 EL1=1 EL2=1 EL3=1 NC=A

\*

LINE NODES 473 585 584  
LINE NODES 468 530 529  
LINE NODES 466 508 507  
LINE NODES 464 486 485  
GVOLUME 1234 1230 585 473 1235 1231 530 468 EL1=1 EL2=1 EL3=4 NC=N  
LINE NODES 530 508 890  
GVOLUME 1235 1231 530 468 1236 1232 508 466 EL1=1 EL2=1 EL3=1 NC=A  
LINE NODES 508 486 908  
GVOLUME 1236 1232 508 466 1237 1233 486 464 EL1=1 EL2=1 EL3=1 NC=A

\*

LINE NODES 585 587 586  
LINE NODES 530 532 531  
LINE NODES 508 510 509  
LINE NODES 486 488 487  
GVOLUME 1230 948 587 585 1231 947 532 530 EL1=1 EL2=1 EL3=4 NC=N  
GVOLUME 1231 947 532 530 1232 946 510 508 EL1=1 EL2=1 EL3=1 NC=A  
GVOLUME 1232 946 510 508 1233 945 488 486 EL1=1 EL2=1 EL3=1 NC=A

\*COORDINATES FOR THE REST OF THE HEADER ARE DEFINED

SYSTEM N=0

COORDINATES/ ENTRIES	NODE	X	Y	Z
	1366	9.09	6.32	0
	1367	9.09	6.32	2.25
	1368	7.86	4.67	0
	1369	7.86	4.67	2.25
	1370	6.9	6.79	0
	1371	6.9	6.79	2.25
	1372	6.644	4.85	0
	1373	6.644	4.85	2.25
	1374	4.91	6.37	0
	1375	4.91	6.37	2.25
	1376	5.39	4.6	0
	1377	5.39	4.6	2.25
	1378	3.16	5.575	0
	1379	3.16	5.575	2.25
	1380	4.3	4.057	0
	1381	4.3	4.057	2.25
	1382	1.93	4.61	0
	1383	1.93	4.61	2.25
	1384	3.31	3.33	0
	1385	3.31	3.33	2.25
	1386	.77	3.03	0
	1387	.77	3.03	2.25
	1388	2.53	2.356	0
	1389	2.53	2.356	2.25
	1390	.17	1.55	0
	1391	.17	1.55	2.25
	1392	2.046	1.22	0
	1393	2.046	1.22	2.25
	1394	0	0	0
	1395	0	0	2.25
	1396	1.87	0	0
	1397	1.87	0	2.25
	1398	8.27	5.22	0
	1399	8.27	5.22	2.25
	1400	8.065	4.945	0

1401 8.065 4.945 2.25

\*THE MESH FOR THE REST OF THE HEADER IS GENERATED

GVOLUME 1238 1230 1231 1239 1366 1367 1399 1398 1401 1400 1401 1369 1368 1372 1373 1377  
GVOLUME 1239 1231 1232 1240 1398 1399 1401 1400 1401 1369 1368 1372 1373 1377 1377  
GVOLUME 1240 1232 1233 1241 1400 1401 1369 1368 1372 1373 1377 1377 1377 1377 1377  
GVOLUME 1367 1366 1370 1371 1369 1368 1372 1373 1376 1376 1376 1376 1376 1376 1376 1376  
GVOLUME 1371 1370 1374 1375 1373 1372 1376 1377 1377 1377 1377 1377 1377 1377 1377 1377  
GVOLUME 1375 1374 1378 1379 1377 1376 1380 1381 1381 1381 1381 1381 1381 1381 1381 1381  
GVOLUME 1379 1378 1382 1383 1381 1380 1384 1385 1385 1385 1385 1385 1385 1385 1385 1385  
GVOLUME 1383 1382 1386 1387 1385 1384 1388 1389 1389 1389 1389 1389 1389 1389 1389 1389  
GVOLUME 1387 1386 1390 1391 1389 1388 1392 1393 1392 1392 1392 1392 1392 1392 1392 1392  
GVOLUME 1391 1390 1394 1395 1393 1392 1396 1397 1397 1397 1397 1397 1397 1397 1397 1397

\*THE NODES AT THE CENTER OF THE TUBES ARE FIXED

BOUNDARIES 111111 TYPE=NODES/949 STEP 1 TO 956

\*THE NODE AT THE ORIGIN IS FIXED

BOUNDARIES 111111 TYPE=NODES/1892

\*THE NODES ABOVE THE ORIGIN ARE ONLY ALLOWED TO ROLL IN THE X-DIRECTION

BOUNDARIES 011111 TYPE=NODES

932 1015 1018 1023 1026 1031 1034 1039 931 1043 930 1046 929

1895 1902 1906 1913 1917 1924 1928 1935 1939 1946 1950 1956

\*THE NODES IN THE Y=0 PLANE ARE CONSTRAINED TO ROLL ONLY IN THAT PLANE

BOUNDARIES 010111 TYPE=NODES

936 1013 1049 928 961 1051 966 1017 1053 1054 973 1059 978 1025 1061 1062  
985 1067 990 1033 1069 1070 997 1075 935 1041 1077 927 1004 1079 934 1044  
1080 926 1009 1082 933 1047 1083 925 1394 1395 1891 1893 1894 1896 1900  
1901 1903 1904 1905 1907 1911 1912 1914 1915 1916 1918 1922 1923 1925 1926  
1927 1929 1933 1934 1936 1937 1938 1940 1944 1945 1947 1948 1949 1951 1396  
1397 1955 1957

\*THE NODES IN THE Z=0 PLANE ARE CONSTRAINED TO ROLL ONLY IN THAT PLANE

BOUNDARIES 001111 TYPE=NODES

1	2	3	4	5	6	7	8	9	10	11	12	13	14	15	16	17	18	19	20	21	22	23	24	25	26	27	28	29	30	31	32	33	34	35	36	37	38	39	40	41	42	43	44	45	46	47	48	49	50																																																																																																																																																																																																																																																																																																																																																																																																					
61	72	83	94	105	116	127	133	136	139	142	145	148	151	154	157	160	163	166	169	175	181	184	187	190	193	196	199	202	205	208	211	214	217	220	223	226	229	232	235	241	247	250	253	259	262	265	268	271	274	277	280	283	286	289	292	295	301	307	310	313	316	319	325	328	331	334	337	343	349	352	355	361	367	370	373	376	379	385	391	394	397	403	409	412	415	418	421	424	427	430	433	436	439	442	445	448	451	454	457	460	463	464	465	466	467	468	469	470	471	472	473	479	490	501	512	523	534	545	556	567	578	589	595	598	601	604	607	610	613	619	625	628	631	637	643	646	649	652	655	661	667	670	673	679	685	688	691	694	697	703	709	712	715	721	727	730	733	736	739	742	745	748	751	754	757	763	769	772	775	781	787	790	793	796	799	805	811	814	817	823	829	832	835	838	841	847	853	856	859	865	871	874	877	880	883	886	889	892	895	898	901	904	907	910	913	916	919	922	941	942	943	946	947	948	949	950	1014	1016	1020	1022	1024	1028	1030	1032	1036	1038	1040	1042	1045	1048	1055	1063	1071	1122	1123	1124	1126	1128	1130	1131	1132	1134	1136	1138	1139	1140	1142	1144	1146	1147	1148	1150	1151	1153	1154	1156	1159	1163	1167	1174	1176	1179	1182	1184	1187	1190	1192	1195	1198	1200	1202	1204	1206	1210	1216	1222	1234	1235	1236	1237	1279	1280	1281	1283	1285	1287	1288	1289	1291	1293	1295	1296	1297	1299	1301	1303	1304	1305	1307	1308	1310	1311	1313	1320	1328	1336	1403	1406	1409	1412	1415	1418	1421	1425	1429	1433	1437	1441	1445	1448	1451	1454	1457	1460	1463	1466	1469	1472	1475	1478	1482	1486	1489	1493	1497	1500	1504	1508	1511	1515	1519	1522	1526	1530	1533	1536	1539	1542	1545	1548	1552	1556	1559	1563	1567	1570	1574	1578	1581	1585	1589	1592	1596	1600	1603	1606	1609	1612	1615	1618	1622	1626	1629	1633	1637	1640	1644	1648	1651	1655	1659	1662	1666	1670	1673	1676	1679	1682	1685	1688	1692	1696	1699	1703	1707	1710	1714	1718	1721	1725	1729	1732	1736	1740	1743	1746	1749	1752	1755	1758	1762	1766	1769	1773	1777	1780	1784	1788	1791	1795	1799	1802	1806	1810	1813	1816	1819	1822	1825	1828	1832	1836	1839	1843	1847	1850	1854	1858

1861 1865 1869 1872 1876 1880 1883 1886 1889 1895 1909 1920 1931 1942 1953  
\*THE INTERNAL PRESSURE LOAD IS APPLIED

LOADS ELEMENT

1 -2 700

STEP 1 TO

120 -2 700

55 -3 700

STEP 1 TO

60 -3 700

115 -3 700

STEP 1 TO

120 -3 700

126 -3 700

STEP 6 TO

192 -3 700

203 -2 700

204 -2 700

215 -3 700

STEP 12 TO

287 -3 700

216 -3 700

STEP 12 TO

288 -3 700

\*

CONSTRAINTS

\*THE FOLLOWING CONSTRAINTS ARE NECESSARY BECAUSE COORDINATES WERE

\*DUPLICATED IN THE GENERATION OF THE MESH FOR THE HEADER AT THE

\*BOUNDARY OF THE TUBES

968 1 1019 1

968 2 1019 2

968 3 1019 3

1020 1 1055 1

1020 2 1055 2

1056 1 1091 1

1056 2 1091 2

1056 3 1091 3

1127 1 1092 1

1127 2 1092 2

1127 3 1092 3

1159 1 1128 1

1159 2 1128 2

967 1 1160 1

967 2 1160 2

967 3 1160 3

980 1 1027 1

980 2 1027 2

980 3 1027 3

1028 1 1063 1

1028 2 1063 2

1064 1 1099 1

1064 2 1099 2

1064 3 1099 3

1135 1 1100 1

1135 2 1100 2

1135 3 1100 3

1163 1 1136 1

1163 2 1136 2

979 1 1164 1

979 2 1164 2

979 3 1164 3

992 1 1035 1  
992 2 1035 2  
992 3 1035 3  
1036 1 1071 1  
1036 2 1071 2  
1072 1 1107 1  
1072 2 1107 2  
1072 3 1107 3  
1143 1 1108 1  
1143 2 1108 2  
1143 3 1108 3  
1167 1 1144 1  
1167 2 1144 2  
991 1 1168 1  
991 2 1168 2  
991 3 1168 3  
1158 1 1177 1  
1158 2 1177 2  
1158 3 1177 3  
1179 1 1210 1  
1179 2 1210 2  
1125 1 1209 1  
1125 2 1209 2  
1125 3 1209 3  
1211 1 1248 1  
1211 2 1248 2  
1211 3 1248 3  
1284 1 1249 1  
1284 2 1249 2  
1284 3 1249 3  
1320 1 1285 1  
1320 2 1285 2  
1352 1 1321 1  
1352 2 1321 2  
1352 3 1321 3  
1178 1 1353 1  
1178 2 1353 2  
1178 3 1353 3  
1162 1 1185 1  
1162 2 1185 2  
1162 3 1185 3  
1187 1 1216 1  
1187 2 1216 2  
1133 1 1215 1  
1133 2 1215 2  
1133 3 1215 3  
1217 1 1256 1  
1217 2 1256 2  
1217 3 1256 3  
1292 1 1257 1  
1292 2 1257 2  
1292 3 1257 3  
1328 1 1293 1  
1328 2 1293 2  
1356 1 1329 1  
1356 2 1329 2  
1356 3 1329 3  
1186 1 1357 1  
1186 2 1357 2  
1186 3 1357 3

1166 1 1193 1  
1166 2 1193 2  
1166 3 1193 3  
1195 1 1222 1  
1195 2 1222 2  
1141 1 1221 1  
1141 2 1221 2  
1141 3 1221 3  
1223 1 1264 1  
1223 2 1264 2  
1223 3 1264 3  
1300 1 1265 1  
1300 2 1265 2  
1300 3 1265 3  
1336 1 1301 1  
1336 2 1301 2  
1360 1 1337 1  
1360 2 1337 2  
1360 3 1337 3  
1194 1 1361 1  
1194 2 1361 2  
1194 3 1361 3  
**\*THE FOLLOWING CONSTRAINTS DEFINE THE CONTACT SURFACES**  
585 2 552 2  
585 3 552 3  
586 2 553 2  
586 3 553 3  
587 2 554 2  
587 3 554 3  
588 2 555 2  
588 3 555 3  
589 2 556 2  
590 2 557 2  
590 3 557 3  
591 2 558 2  
591 3 558 3  
592 2 559 2  
592 3 559 3  
593 2 560 2  
593 3 560 3  
594 2 561 2  
594 3 561 3  
473 2 470 2  
584 2 551 2  
584 3 551 3  
1323 2 759 2  
1323 3 759 3  
1354 2 760 2  
1354 3 760 3  
1180 2 761 2  
1180 3 761 3  
1181 2 762 2  
1181 3 762 3  
1182 2 763 2  
1212 2 764 2  
1212 3 764 3  
1213 2 765 2  
1213 3 765 3  
1250 2 766 2  
1250 3 766 3

1251	2	767	2
1251	3	767	3
1286	2	768	2
1286	3	768	3
1287	2	757	2
1322	2	758	2
1322	3	758	3
1331	2	801	2
1331	3	801	3
1358	2	802	2
1358	3	802	3
1188	2	803	2
1188	3	803	3
1189	2	804	2
1189	3	804	3
1190	2	805	2
1218	2	806	2
1218	3	806	3
1219	2	807	2
1219	3	807	3
1258	2	808	2
1258	3	808	3
1259	2	809	2
1259	3	809	3
1294	2	810	2
1294	3	810	3
1295	2	799	2
1330	2	800	2
1330	3	800	3
1339	2	843	2
1339	3	843	3
1362	2	844	2
1362	3	844	3
1196	2	845	2
1196	3	845	3
1197	2	846	2
1197	3	846	3
1198	2	847	2
1224	2	848	2
1224	3	848	3
1225	2	849	2
1225	3	849	3
1266	2	850	2
1266	3	850	3
1267	2	851	2
1267	3	851	3
1302	2	852	2
1302	3	852	3
1303	2	841	2
1338	2	842	2
1338	3	842	3
123	2	90	2
123	3	90	3
124	2	91	2
124	3	91	3
125	2	92	2
125	3	92	3
126	2	93	2
126	3	93	3
127	2	94	2

128	2	95	2
128	3	95	3
129	2	96	2
129	3	96	3
130	2	97	2
130	3	97	3
131	2	98	2
131	3	98	3
132	2	99	2
132	3	99	3
11	2	8	2
122	2	89	2
122	3	89	3
969	2	297	2
969	3	297	3
970	2	298	2
970	3	298	3
971	2	299	2
971	3	299	3
1021	2	300	2
1021	3	300	3
1022	2	301	2
1057	2	302	2
1057	3	302	3
1058	2	303	2
1058	3	303	3
1093	2	304	2
1093	3	304	3
1094	2	305	2
1094	3	305	3
1129	2	306	2
1129	3	306	3
1130	2	295	2
1161	2	296	2
1161	3	296	3
981	2	339	2
981	3	339	3
982	2	340	2
982	3	340	3
983	2	341	2
983	3	341	3
1029	2	342	2
1029	3	342	3
1030	2	343	2
1065	2	344	2
1065	3	344	3
1066	2	345	2
1066	3	345	3
1101	2	346	2
1101	3	346	3
1102	2	347	2
1102	3	347	3
1137	2	348	2
1137	3	348	3
1138	2	337	2
1165	2	338	2
1165	3	338	3
993	2	381	2
993	3	381	3
994	2	382	2

994	3	382	3
995	2	383	2
995	3	383	3
1037	2	384	2
1037	3	384	3
1038	2	385	2
1073	2	386	2
1073	3	386	3
1074	2	387	2
1074	3	387	3
1109	2	388	2
1109	3	388	3
1110	2	389	2
1110	3	389	3
1145	2	390	2
1145	3	390	3
1146	2	379	2
1169	2	380	2
1169	3	380	3
283	2	1124	2
284	2	962	2
284	3	962	3
285	2	963	2
285	3	963	3
286	2	1016	2
287	2	1052	2
287	3	1052	3
288	2	1088	2
288	3	1088	3
325	2	1132	2
326	2	974	2
326	3	974	3
327	2	975	2
327	3	975	3
328	2	1024	2
329	2	1060	2
329	3	1060	3
330	2	1096	2
330	3	1096	3
367	2	1140	2
368	2	986	2
368	3	986	3
369	2	987	2
369	3	987	3
370	2	1032	2
371	2	1068	2
371	3	1068	3
372	2	1104	2
372	3	1104	3
409	2	1148	2
410	2	998	2
410	3	998	3
411	2	999	2
411	3	999	3
412	2	1040	2
413	2	1076	2
413	3	1076	3
414	2	1112	2
414	3	1112	3
745	2	1281	2

746 2 1317 2  
746 3 1317 3  
747 2 1175 2  
747 3 1175 3  
748 2 1176 2  
749 2 1208 2  
749 3 1208 3  
750 2 1245 2  
750 3 1245 3  
787 2 1289 2  
788 2 1325 2  
788 3 1325 3  
789 2 1183 2  
789 3 1183 3  
790 2 1184 2  
791 2 1214 2  
791 3 1214 3  
792 2 1253 2  
792 3 1253 3  
829 2 1297 2  
830 2 1333 2  
830 3 1333 3  
831 2 1191 2  
831 3 1191 3  
832 2 1192 2  
833 2 1220 2  
833 3 1220 3  
834 2 1261 2  
834 3 1261 3  
871 2 1305 2  
872 2 1341 2  
872 3 1341 3  
873 2 1199 2  
873 3 1199 3  
874 2 1200 2  
875 2 1226 2  
875 3 1226 3  
876 2 1269 2  
876 3 1269 3

\*PORTIONS OF THE MODEL ARE DEFINED FOR GRAPHICS

EZONE TUBE1  
1 2 STEP 1 TO 60

EZONE TUBE2  
61 62 STEP 1 TO 120

EZONE TUBE3  
121 122 STEP 1 TO 156

EZONE TUBE4  
157 158 STEP 1 TO 192

ZZONE COMBO1 TUBE1 TUBE3  
ZZONE COMBO2 TUBE2 TUBE4  
ZZONE COMBO3 TUBE1 TUBE2 TUBE3 TUBE4

EZONE LOAD  
126 STEP 6 TO 192 203 STEP 12 TO 287 204 STEP 12 TO 288  
ZZONE LOADING TUBE1 TUBE2 LOAD

## LIST OF REFERENCES

1. Kaufmann, J.W., *Stress Analysis of the LHA-1 Class Superheater Header by Finite Element Method, Master's Thesis*, Naval Postgraduate School, California, June 1987.
2. ADINA Engineering, *ADINA-IN Users Manual, Report ARD 84-6*, ADINA R&D, Inc., Massachusetts, December 1984.
3. ADINA Engineering, *ADINA Theory and Modeling Guide, Report ARD 84-4*, ADINA R&D, Inc., Massachusetts, December 1984.
4. Bathe, K.J., *Finite Element Procedures in Engineering Analysis*, Prentice Hall, Inc., New Jersey, 1982.
5. ADINA Engineering, *ADINAT Users Manual, Report ARD 84-2*, ADINA R&D, Inc., Massachusetts, December 1984.
6. ADINA Engineering *ADINA-PLOT Users Manual, Report ARD 84-3*, ADINA R&D, Inc., Massachusetts, December 1984.
7. Gere, J.M. and Timoshenko, S.P., *Mechanics of Materials*, PWS Publishers, Boston, Massachusetts, 1984.
8. Ugural, A.C. and Fenster, S.K., *Advanced Strength and Applied Elasticity, The SI Version*, Elsevier North Holland, Inc., New York, 1981.

## INITIAL DISTRIBUTION LIST

	No. Copies
1. Defense Technical Information Center Cameron Station Alexandria, VA 22304-6145	2
2. Library, Code 0142 Naval Postgraduate School Monterey, CA 93943-5002	2
3. Chairman, Code 69Hy Department of Mechanical Engineering Naval Postgraduate School Monterey, CA 93943-5000	1
4. Professor Gilles Cantin, Code 69Ci Department of Mechanical Engineering Naval Postgraduate School Monterey, CA 93943-5000	4
5. Professor David Salinas, Code 69Sa Department of Mechanical Engineering Naval Postgraduate School Monterey, CA 93943-5000	1
6. Professor C. Lee, Code 69Le Department of Mechanical Engineering Naval Postgraduate School Monterey, CA 93943-5000	1
7. Professor Edward L. Wilson Structural Engineering Division Department of Civil Engineering University of California, Berkeley Berkeley, CA 94720	1
8. Professor K.J. Bathe Department of Mechanical Engineering Massachusetts Institute of Technology 77 Massachusetts Avenue Cambridge, MA 02139	1
9. Dr. Jean Louis Batoz U.T.C. Universite de Technologie 60206 Compiegne Cedex, FRANCE	1

- |     |  |   |
|-----|--|---|
| 10. | Professor Thomas Hughes<br>Division of Applied Mechanics<br>Room 283 Durand<br>Stanford, CA 94305  | 1 |
| 11. | Dr. Rem Jones, Code 172<br>David W. Taylor Naval Ship<br>Research and Development Center<br>Bethesda, MD 20084                                   | 1 |
| 12. | Mr. Craig Fraser, Code 2814<br>David W. Taylor Naval Ship<br>Research and Development Center<br>Annapolis Laboratory<br>Annapolis, MD 21402-5067 | 1 |
| 13. | CDR Lael Easterling, USN, Code 56X6<br>NAVSEA Boiler Engineering Division<br>NAVSEA Headquarters<br>Washington, DC 20362-5101                    | 1 |
| 14. | Dr. Alan Kushner, Code 4325<br>Office Of Naval Research<br>360 North Quincy Street<br>Arlington, VA 22217  | 1 |
| 15. | Mr. Joseph Carrado, Code 1702<br>David W. Taylor Naval Ship<br>Research and Development Center<br>Bethesda, MD 20034                             | 1 |
| 16. | R.A. Langworthy<br>Applied Technology Laboratories<br>U.S. Army Research and Technology Laboratory<br>Fort Eustis, VA 23604                      | 1 |
| 17. | LT Jon W. Kaufmann, USN<br>10 Sycamore Drive<br>Roslyn, NY 11576   | 1 |
| 18. | LCDR Doyle R. Kitchin, USN<br>RT 1, BOX 122-LL<br>Prague, OK 74864   | 5 |

END

DATED

FILM

8-88

DTIC